To the Graduate Council:

We are submitting herewith a thesis written by Bethsheba Lavoie entitled “Transport of explosive residue surrogates in saturated porous media.” I have examined the final electronic copy of this thesis for form and content and recommend that it be accepted in partial fulfillment of the requirements for the degree of Master of Science, with a major in Geology.

Larry D. McKay
Major Professor

Melanie A. Mayes
Co-Major Professor

I have read this thesis
and recommend its acceptance:

Edmund Perfect

Accepted for the Council:

Carolyn R. Hodges
Vice Provost and Dean
of the Graduate School

(Original signatures are on file with official student records.)

Transport of Explosive Residue Surrogates in Saturated Porous Media

A Thesis Presented for
The Master of Science
Degree
The University of Tennessee, Knoxville

Bethsheba Lavoie
December 2010

Copyright © 2010 by Bethsheba Lavoie
All rights reserved.

For my grandfather

Robert Van Guilder

Acknowledgments

I would like to express my gratitude to Drs. Larry McKay and Melanie Mayes, my thesis co-supervisors, for their guidance throughout my degree program. I would like to give special thanks to Dr. Ed Perfect for serving on my thesis committee, but moreover, for always making time to help and to listen. I would also like to thank Drs. Steven Minkin and John Biggerstaff for all of their work and for sharing their expertise. Thanks also to Balaji Bharatwaj, Dan Williams, Guoping Tang, Scott Moser, Doug Fielden, Larry Smith, and Galina Melnichenko for their support of my research. To my friends and fellow students, Peter Knappett, Andrew Moore, Keshia Koehn, Bob Hunter, and Ankur Roy, heartfelt thanks for your advice and encouragement. And to my greatest love and inspiration, Ganesh Kamath, thank you for making it all worthwhile.

I would like to express my appreciation to the Strategic Environmental Research and Development Program (SERDP) for providing funding for this project.

Abstract

Contamination of soils by munitions constituents is pervasive on Department of Defense operational ranges. Low-order detonations result in the heterogeneous distribution of explosives residues (ER) at shallow depths. At a limited number of ranges ER contamination of groundwater has been observed.

Previous studies have shown that the downward migration of colloid-sized contaminants can significantly impact groundwater quality. The goal of this study was to investigate if colloid transport plays a role in the migration of ER contaminants. Our primary objective was to determine the transport potential of fine (<5 um) ER particles under ideal conditions for colloid transport. A secondary objective was to develop a direct detection method for the identification and quantitative analysis of particulate ER.

A series of saturated transport experiments were conducted in columns (2x20 cm) packed with clean sand. 2,6- Dinitrotoluene was used as a surrogate for explosives chemicals. Experiments were conducted with both particulate and dissolved-phase DNT. Bromide and microspheres tracers were also used to characterize nonreactive transport. Particulate tracers were applied to the columns, either suspended in the influent solution, or directly to the top layer of sand, in order to more realistically replicate field conditions. Experimental results indicate that DNT movement through the columns occurred as a combination of solid and dissolved phase transport. Concentration differences between unfiltered and filtered samples indicate that particulate DNT accounted up to 30% of the total mass recovered in the effluent.

Contents

Chapter 1: Introduction 1

Chapter 2: Methods and Materials 7

Column Experiments 7

Particulate Tracers 9

Preparation and particle size analysis of solid-phase DNT 9
Microspheres 10
Preparation of Dissolved-phase DNT Solution 10

Detection Methods 10

EPA Method 8515 10
EPA Method 8330 12
Immunolabeling/Chemical Staining 13
Transport Modeling 14

Chapter 3: Results 15

DNT Particle Size Analysis 15

Transport Experiments 15

Microsphere Tracer Experiments 15
DNT Particulate Tracer Experiments 15
Dissolved-phase DNT experiment 20
Bromide Tracer and Modeling Results 21
Detection Method Development 21

Immunolabeling 21
Chemical staining 21
Chapter 4: Discussion 23

Development of Experimental Methods 23

DNT particle size and flocculation 23

Methods for Detecting DNT 24

Labeling particulate DNT 24
Comparison of analytical methods 8515 and 8330 25
DNT Tracer Experiments 26

Dissolved phase experiment 26
DNT Suspension Experiment 26
Particulate DNT surface application experiments 28
Chapter 5: Conclusions & Recommendations 30

Methods for the direct detection of particulate explosives residues 30

Transport of particulate explosives residues 30

References 32
Appendix A 42
Appendix B 70
Appendix C 89
Vita 97

List of Figures

Figure 1- Experimental set-up 44
Figure 2 – Particle size distribution 45
Figure 3– Particle size analysis images 46
Figure 4– DNT particle size analysis 47
Figure 5 - Effluent results for suspended particulate DNT experiment 1F-P 48
Figure 6 - Effluent results for particulate DNT surface application experiment 2F-P 49
Figure 7 – DNT distribution in sand samples from particulate DNT surface application experiment 2F-P. 50
Figure 8 –Comparison of effluent results for suspended DNT experiment 1F-P and DNT particulate surface application experiment 2F-P 51
Figure 9- DNT concentrations for unfiltered and filtered effluent samples from DNT particulate surface application experiments in fine (3F-P) and medium (5M) sand. 52
Figure 10 - Comparison of effluent results for particulate DNT surface application experiments in fine (4F) and coarse (5M) sand 53
Figure 11- Ratio of filtered to unfiltered DNT concentrations in effluent samples from DNT particulate surface application experiments in fine (4F) and medium (5M) sand. 54
Figure 12 – Comparison of the DNT distribution in sand samples from particulate DNT surface application experiments in fine (4F) and coarse (5M) sand 55
Figure 13 – Testing the reproducibility of analytical method 8515 56
Figure 14 – Comparison of effluent results for all four particulate DNT surface application experiments 57
Figure 15 – Comparison of the DNT distribution in sand samples from particulate DNT surface application experiments 2F-P, 4F, and 5M 58
Figure 16 –Comparison of results for 4F effluent samples analyzed by methods 8515 and 8330. 59
Figure 17 - DNT concentrations for filtered effluent samples from dissolved phase experiment 6F 60
Figure 18 - DNT distribution in sand samples from dissolved phase experiment 6F 61
Figure 19 – Comparison of effluent results for dissolved phase DNT experiment 6F and particulate DNT surface application experiment 4F, both in fine sand. 62
Figure 20 - Time series of images of DNT powder reacting with different TBAH concentrations 63
Figure 21 - Image of a sand sample from column experiment 2F-P 64
Figure 22 – Image of DNT particle aggregates in the influent solution with 1% BSA 65

List of Tables

Table 1: Chemical properties of Composition B constituents and ER surrogate 67
Table 2: Summary of column transport experimental conditions..... 68
Table 3: Mass balance results for DNT tracer experiments..... 69

Chapter 1: Introduction

Contamination of near surface soil by explosives residues (ER) is a pervasive problem at former/active Department of Defense (DoD) firing ranges. The use of high explosives during training exercises leaves significant concentrations of ER particles in soils which can subsequently infiltrate underlying aquifer systems. At a limited number of ranges, ER groundwater plumes are observed (Clausen et al., 2006). Due to their toxicity and carcinogenicity, ER contamination of groundwater poses both ecological and public health risks (ATSDR, 2010).

The extent of ER contamination on a given range is largely dependent on the level of detonation. Partially exploded or low-order detonations (defined as < 100% of the round expended) act as randomly distributed sources of potentially leachable ER (Jenkins et al. 2006). Duds and/or low-order detonations can account for up to 4.4 percent of total detonations (Morley et al., 2006). In ER samples collected from blown-in-place, low-order detonations, Taylor et al. (2006) found that particle size distribution ranges from several centimeters to < 250 μm in diameter.

One of the most common explosives currently employed by the DoD is Composition B (CB) (Taylor et al., 2006). The main constituents of CB are: 2,4,6-trinitrotoluene (TNT) and hexahydro-1,3,5-trinitro-1,3,5-triazine (RDX), which are proportionally by mass 39.5% and 59.5%, respectively, with an additional 1% paraffin wax. Octahydro-1,3,5,7-tetranitro-1,3,5,7-tetrazocine (HMX) is also often present as an impurity in the RDX (up to 10%). Batch and column sorption experiments indicate that RDX and HMX are expected to be transported in groundwater, while TNT is somewhat less likely to be transported because of its higher distribution coefficient (K_d), particularly in clay-rich soils (**Table 1**) (Dontsova, et al., 2006; Clausen et al., 2006). All three chemical constituents have relatively low solubility (**Table 1**). The solubility values, although low, are still substantially above the health advisory (HA) guidance levels for all three, 0.002 mg/L for TNT and RDX and 0.4 mg/L for HMX (EPA, 2009a). Hence, even with limited solubility CB residue is believed to pose a public health concern.

Although ER contamination of soils on firing ranges has been studied and documented extensively (Jenkins et al., 2006), contamination of groundwater with CB has been reported for only a few locations in United States and Canada. At Camp Edwards, located on Cape Cod in Massachusetts, both TNT and RDX have been detected in the groundwater (Clausen et al., 2006). Hydrogeological characteristics of the site include sandy soils with low percentages of clay/organic material, high rainfall, and high aquifer flow rates, which are typical to sites that are vulnerable to groundwater contamination. The results of extensive soil sampling at Camp Edwards indicate that TNT and RDX contamination is limited to widely dispersed, shallow sources. The TNT detected in groundwater appears to be limited to within 100 feet of identified source areas, likely due to sorption and degradation. However, a nearly two mile long RDX plume has been delineated using groundwater samples, indicating its migration through a relatively thick (~ 35 meters) vadose zone to the water table (Clausen et al, 2006). Low concentrations (< 1 μg/L) of RDX have also been detected in groundwater samples from Ft. Lewis, Washington (Jenkins et al., 2001). The soils at Ft. Lewis are reported to be coarse gravelly sands with low total organic content. To the best of the author's knowledge, HMX contamination of groundwater has not yet been reported for US military ranges, but has been observed in Canada. In a field investigation of firing ranges at Canadian Forces Base (CFB) Valcartier in Quebec, Thiboutot et al. (1998) detected HMX in the groundwater there as well as TNT and RDX. The soil at CFB Valcartier is sandy and well-drained, similar to Camp Edwards, but the water table is not as deep at only ~3.5 meters.

There are more than 200 active and former DoD installations located in the United States, many of which have operational ranges (Military.com). Each branch of the U.S. military has its own internal program responsible for the environmental assessment of operational ranges (e.g. the Army's Operational Range Assessment Program [ORAP]). In these programs, the prioritization of which contaminant types to investigate are necessarily driven by many factors including the perceived level of threat to public health and the environment, as well as regulatory concerns. As mentioned above, the EPA does not currently regulate CB compounds in groundwater. Moreover, prior to the discovery of groundwater contamination at Camp Edwards, it was widely believed that these chemicals did not pose a great threat to groundwater resources. Because of

this, groundwater monitoring for the presence of CB compounds is not widely practiced at DoD facilities. Based upon the detection of ER in the few monitored locations, it is possible that the prevalence of ER contamination in groundwater could be much greater than present data suggest.

Much progress has been made towards expanding our knowledge of the chemical/ physical properties of explosives compounds. The most common conceptual models in the literature are based on the assumption that solid explosives residues are deposited at or near the ground surface, are then dissolved by precipitation, and leached through the vadose zone as a dissolved phase (Hewitt et al, 2005; Clausen et al, 2006). However, efforts to develop predictive fate and transport models to determine the potential impact of training range activities have proven complicated. For example at Camp Edwards, RDX concentrations in the groundwater exceed anticipated levels based on measured concentrations in the vadose soils and the solubility/partition coefficients of the chemical (Clausen et al, 2006). In addition to near surface dissolution and leaching of dissolved phase ER, transport of ER chemicals in the solid phase, as colloids or as dissolved phase compounds adsorbed to colloidal soil materials (i.e. clays/organic matter) could be contributing to groundwater contamination.

The movement of colloids can play a significant role in the transport of contaminants. Colloidal contaminants (e.g. bacteria, viruses) or contaminants adsorbed to natural colloids (e.g. clay particles, organic material) are often transported faster in groundwater then dissolved constituents (McCarthy and Zachara, 1989). This is because colloids tend to be size-excluded from the slow flow regimes of fine pore structure. The transport of colloids can be further augmented by the presence of soil macropores, which act as preferential pathways for the vertical migration. Because colloids are excluded by size from diffusion into fine-grained matrices, their movement in such soils is restricted to macropores where groundwater velocities can greatly exceed those expected based on bulk hydraulic conductivity (McCarthy and McKay, 2004). In laboratory and field scale tracer experiments using microspheres in fractured rock, Becker et al. (1999) found that the surrogate colloids typically arrived before solute tracers. Poulsen et al. (2006) made similar observations in their experimental study comparing the transport of a bromide tracer and natural soil colloids in undisturbed soil columns. Modeling results for their research indicate that colloid transport velocity is two to three times faster than

that of the bromide (Poulsen et al., 2006). Both studies attribute the higher relative velocities of the colloids to size exclusion.

Colloid mobility is also greatly influenced by soil moisture content. Under partially-saturated conditions colloid retention is enhanced by sorption to the air-water interface (Sirivithayapakorn and Keller, 2003). In addition, with significantly decreased moisture content, flow is restricted to thin films along grain surfaces, thereby increasing the likelihood of physical retention as the diameter of the colloid and the flow path converge (Wan and Tokunaga, 1997). Furthermore, colloids entrained in vadose zone soils can be remobilized as the moisture content increases. Infiltration during storm events often results in higher flow rates and a reduction in pore water ionic strength, both of which typically increase colloid mobilization (DeNovio et al., 2004; Cey et al. 2009). Zhuang et al. (2009) demonstrated that colloids in partially-saturated porous media can be mobilized during both periods of infiltration and subsequent drainage. Field and laboratory studies have shown that particle concentrations in pore water peak during the initial period of infiltration events (El-Farhan et al., 2000; Ryan et al., 2008, Shang et al., 2008).

Colloid-sized explosives particulates or explosives compounds adsorbed to soil colloids could potentially be mobilized under conditions of saturated or temporarily saturated flow. Once mobilized, they could travel directly to the water table or be retained deeper in the vadose zone. From there, they could remain as persistent sources of dissolved-phase contamination or be remobilized during subsequent storm events. The optimum colloid size for transport depends on the characteristics of the porous media. In transport experiments using sand columns, Bradford and Bettahar (2006) demonstrate that the particle size to the median grain size ratio (d_c/d_{50}) is an important factor affecting colloid transport, with greater mass colloid fraction recovered with lower d_c/d_{50} values. In dual porosity media, such as fractured clay, the optimum colloid size for transport appears to have both an upper and a lower limit. Cumbie and McKay (1999) found with experiments in undisturbed shale saprolite that breakthrough was greatest for microspheres between 1.0 μm to 0.5 μm in diameter, with lower recover for the larger (4.25 μm) and smaller (0.05 μm and 0.1 μm) sizes. Post-experimental analyses of column material samples detected retained microspheres mostly along fracture surface but also some within the fine grained matrix of the shale, suggesting the smaller spheres were able diffuse into the finer pore structure

(Cumbie and McKay, 1999). Zvikelsey and Weisbord (2006) made similar observations in transport experiments conducted in fractured chalk cores. They found that the smallest size microsphere (0.02 μm) used in the study exhibited the lowest recover in effluent which they also attributed to diffusion into matrix pores.

Very little is known about the properties of small (< 250 μm) explosives residues particles, especially those in the size range expected to be readily transported in soils or aquifer materials. Previous studies examining the size distribution of explosives residues have focused almost exclusively on the centimeter to millimeter pieces as potential point sources of contamination (Jenkins et al. 2006, Taylor et al, 2004). However, the same studies have also reported the occurrence of fine explosives residues (< 250 μm) coincident to the deposition of the larger fragments. In high- and low-order test detonations performed by Taylor et al. (2004) produced a significant number of sub-millimeter sized TNT particles. Of that residue, approximately 10% (low-order) and 67% (high-order) of the mass consisted of < 2 μm particles. As part of a field study that investigated ER distribution on a firing range at Fort Ord in California, Jenkins et al. (1998) analyzed the abundant dust created during homogenization of soil samples. Analytical results for the dust were two to three times higher in concentration than those for the bulk soil, indicating the presence of fine ER particles.

The existing body of colloid transport research generally focuses on colloid facilitated transport of dissolved compounds or transport of non-dissolving biological contaminants such as microbes. Because ER chemicals show little tendency to adsorb to soils, dissolved phase transport facilitated by natural soil colloids seems unlikely. However, given low solubility values it is possible that fine, micron to sub-micron sized, ER particles could be mobilized as colloids. The transport of such fine ER particles as colloids could substantially contribute to the downward migration of explosives compounds through the vadose zone to underlying aquifers.

The primary goal of this study was to develop methods for experimentally assessing the transport of ER in granular porous media. A secondary goal was to determine whether ER particles are likely to be transported by groundwater under conditions of saturated flow in granular sediments. Detection methods for the identification and quantification of ER particulate in sediment were

also tested. The compound 2,6- Dinitrotoluene (DNT) was used as a surrogate for particulate ER. Transport experiments were conducted in fine- and medium-grained sand, using fluorescent latex microspheres and particulate DNT. The particulate tracers were introduced to the columns suspended in the influent or mixed directly into the top layer of sand to mimic field conditions. The presence of particulate ER surrogate in effluent water from the columns was inferred from concentrations difference between filter and unfiltered samples. Transport experiments using dissolved sodium bromide and DNT tracers were also conducted to illustrate the transport of a non-reactive and potentially reactive compound, respectively, for a qualitative comparison to the transport of the particulate tracer.

It was hypothesized that the migration of DNT through the columns would occur as a combination of both dissolved and particulate transport. In addition, DNT was not expected to adsorb strongly to clean sand. Given the above hypotheses, the expected results of the experiments are

- Total DNT concentrations in unfiltered effluent samples should be higher than concentrations in filtered samples due to the presences of particle DNT.

- DNT concentration differences between unfiltered and filtered effluent samples are expected to be greater for experiments using the coarser sand, as retention of the particle DNT in the column material should decrease.

- While DNT is not expected to exhibit chemical retardation, DNT breakthrough will be limited by solubility and dissolution.

- Significant retention of DNT particles in the sand is expected due to physical straining. Post-experiment sand samples should exhibit a decreasing DNT concentration from the top to the bottom of the column.

Chapter 2: Methods and Materials

Column Experiments

A series of saturated flow experiments were conducted utilizing 2 centimeter (cm) diameter x 20 cm long, vertical, clear, polyvinyl chloride (PVC) columns (**Figure 1**, all figures and tables are listed in **Appendix A**). Two different grain sizes of acid-washed Ottawa sand were packed into the columns using a standard tap and fill method (Snyder and Kirkland, 1979). As defined by the ASTM, one is characterized as a medium to fine grained sand (d_{50} = 0.374 mm), herein referred to as "fine sand", and the other is characterized as a medium grained sand (d_{50} = 1.04 mm), herein referred to as "medium sand" (Fetter, 1994). Particle size distribution curves for both sands are presented in **Figure 2**. The porosity of the columns was inferred by the difference between dry and wet mass (**Table 2**).

In each experiment, the column was slowly saturated from the bottom with a background solution of 0.005 M $CaCl_2$ artificial groundwater (AGW). Saturated hydraulic conductivity (K_{sat}) was measured using either a falling head or constant head technique (K_{sat} values provided in **Table 2**). After K_{sat} tests were complete, the influent entry point was switched from the bottom to the top of the column. All experiments were performed using an infusion pump with a constant input (Q_{in}) rate of 400 milliliters per hour (ml/hr). Prior to the introduction of the influent solution and/or particle material, columns were flushed with a minimum of six pore volumes (PV) of AGW.

Three types of transport experiments were conducted:

1. particulate DNT or microsphere tracers introduced in suspension;
2. particulate DNT or microsphere tracers mixed with the top layer of sand ("surface application" experiments);
3. dissolved-phase tracers introduced in solution.

A summary of the materials used and conditions for each experiment is provided in **Table 2**. Two column experiments were conducted using the conventional method of introducing the particulate tracers suspended in the influent solution. These experiments were used to determine the relative mobility of the surrogate explosives residues, as compared to the dissolved tracers and microspheres, and to test the feasibility of the technique in which the particulate tracers are applied directly to the surface of the column. The application of particulate tracers mixed with the top layer of sand is designed to better represent the shallow distribution of ER observed in the field. Dontsova et al. (2006) used a similar method in column experiments using larger (0.25- to 2 mm) Compound B residues. For these experiments flow was temporarily interrupted to apply ER particulate surrogates to the top one cm of sand in the column. After the initial AGW flush, flow was stopped and the top end cap of the column was removed. Approximately 1.5 cubic centimeters of sand was then removed from the column and placed in a weigh boat. A pre-measured quantity of ER particulate surrogate (microspheres or prepared DNT powder) was thoroughly mixed with the sand from the column plus an additional one gram of sand of the same grain size. The top layer of the column was then gently repacked with the ER particulate surrogate/sand mixture, withholding approximately 1 g for later analysis to determine the initial concentration of the ER particulate. Once repacked, a small amount (< 0.5 mL) of background solution was applied directly to the top layer column to ensure completely saturation. Finally, the end cap was replaced and flow resumed, introducing the influent solution. Dissolved-phase tracer experiments were conducted with dissolved-phase surrogate explosive DNT and bromide.

All influent solutions consisted of AGW with 1 gram per liter (g/l) of bovine serum albumin (BSA) added as a particulate dispersant (with the exception of experiment M1). The BSA was added because a preliminary laboratory test (described in results section) showed that DNT particles tended to flocculate in tap water, which would greatly inhibit their transport in the sand columns. For select columns, the influent solution was also supplemented with a conservative tracer [0.001 M Bromide (Br^-)]. An influent pulse of approximately seven PV was introduced to each column followed by a flush of approximately seven PV of plain AGW (with the exception of experiments 4F and 6F which were not flushed). All effluent was captured with a continuous fraction collector. Upon completion of the transport experiments, each saturated column was quickly sealed and frozen to prevent further dissolution of particulate DNT. The freezing process

also facilitates the sectioning of the columns into sub-samples by increasing the cohesion of the sand. Once frozen, the column was sliced into 1 cm sections using a pipe-cutter.

Particulate Tracers

Preparation and particle size analysis of solid-phase DNT

The compound 2,6- dinitrotoluene (DNT) was used as an analog for ER. While not a direct constituent of Compound B (CB), it shares a similar chemical structure and has comparable solubility and distribution coefficient values (**Table 1**). The DNT was obtained from Sigma Aldrich and Ultra Scientific. Three batches (A, B, C) of crystalline DNT were ground to a fine powder using a porcelain mortar and pestle. Batch A was used for column experiments 1F-P and 2F-P. Batch B was used for column experiment 3F-P and for testing of the chemical staining detection method. Batch C was used for column experiments 4F, 5M, and 6F.

The particle size distribution was determined for the three batches of DNT powder using microscopy and image analysis software. Slides were prepared by applying a small (~10 mg) sample of DNT powder on a glass slide, adding 5µl of tap water, and then sandwiching the suspension between the slide and coverslip. Initial observations of the water-DNT suspensions showed that clusters (or flocs) of the finely ground DNT particles quickly formed in the water (**Figure 3A**). A 1% BSA solution was used for the particle size analyses to prevent flocculation. BSA can be used as a dispersant [e.g. in the medical application of carbon nanoparticles (Elgrabli et al, 2007)]. Results from Suttiprasit et al (1992) show that the addition of 1 g of BSA per L of water (with a 0.01 M phosphate buffer of 7 pH) reduces the surface tension of the solution by approximately 20%. Treatment with BSA allowed for a homogeneous suspension of particles in the solution, enabling more accurate analyses of the particle size distribution (**Figure 3B**). Subsequently, BSA was added to the influent solution of the particulate DNT column experiments to prevent the formation of aggregates. It was also added the other column experiments (with the exception of M1) to maintain consistency of experimental conditions.

Transmitted-light brightfield microscopy and automated image analysis software (NIS-Elements v3.0, Nikon, Melville, NY, USA) was used to determine the size distributions of the DNT

particles suspended in the 1% BSA solution. Analytical results were reported in terms of particle equivalent diameter. Assuming a spherical geometry, the equivalent diameter is calculated using the total area of the particle, determined from the two dimensional microscopic image.

Microspheres

Microsphere properties and detection methods used to analyze samples from the microsphere experiments are provided in **Appendix B**.

Preparation of Dissolved-phase DNT Solution

Dissolved-phase DNT was used for one column experiment (6F). A stock solution of DNT was prepared using the solid-phase powder dissolved in AGW. Pure particulate DNT was weighed and placed in a capped plastic conical tube. The DNT was then melted by suspending the tube containing the powder in a flask of water which was gradually heated to 180 degrees Celsius. Simultaneously in another flask, 1 liter of AGW was heated to the same temperature. When the DNT appeared to be completely melted, it was carefully poured from the conical tube into the heated AGW. Then using a glass pipette, the tube was flushed with heated AGW to remove any remaining DNT. The DNT/AGW solution was kept at 180 degrees C while being mixed with a stir bar for several hours. Afterwards, the solution was slowly returned to room temperature. Finally, it was passed through a vacuum filter apparatus with a 0.2 μm pore size nylon filter to remove any remaining DNT particles.

Detection Methods

EPA Method 8515

Selected effluent samples from preliminary DNT experiments (1F-P, 2F-P, 3F-P) were analyzed with EPA Method 8515. Method 8515 is a colorimetric based analysis technique approved by the EPA for screening soil and water for the presence of trinitrotoluene, and other chemically related nitroaromatic compounds, at concentrations >1 ppm (USEPA, 2009b). Method 8515 is generally

performed using test kits that are easily applied in field or bench top settings. While this method is not as quantitatively reliable as other analytical techniques, the cost of the test kits is considerably less (> 10 times) than that of analyses performed by a commercial laboratory (Jenkins & Walsh, 1992).

All 8515 analyses were performed at the University of Tennessee using Ensys® soil test kits, herein referred to as test kits (Strategic Diagnostics). The protocol for aqueous samples, as provided by the manufacturer, is designed for > 1 L sample volumes. For the purposes of this research, it was necessary to adapt the protocol for the small sample volumes (< 4 ml) of effluent collected from the column experiments. In the standard analysis procedure, the effluent sample is vacuum filtered through a membrane (SM Empore SDB-XC) designed to extract the explosives chemical (DNT) from the aqueous solution. The DNT is then eluted from the membrane with acetone and treated with the colorimetric developer for absorbance analysis with a spectrophotometer (Beckman Coulter, model # DU640B).

The purpose of the filtration is to remove the analyte from the solution. The membrane filters supplied with the test kits are designed for >1 L volume samples. Attempts to obtain the SM Empore SDB-XC filter membrane in a syringe cartridge or some other form suitable for small volume samples were unsuccessful. As an alternative to extracting the DNT from the effluent solution through filtration, a vacuum centrifuge was used to evaporate the water from the samples.

Effluent samples in Eppendorf tubes were placed in the vacuum centrifuge. Once the centrifuge achieved full rotational speed, the vacuum pressure was slowly applied. Samples were generally centrifuged for 24 hours, until all water was evaporated, leaving the DNT and any other constituents (CaCl2, NaBr, BSA). The “dry effluent” sample was then dissolved with a 1:25 mixture of developer and acetone and analyzed with the spectrophotometer. Prior to each sample set, spectrophotometer calibration was performed using 1, 5, 15, and 30 ppm concentration DNT solutions. Spectrophotometry analysis was conducted at an absorbance wavelength of 540 nm (A540).

Sand samples from these transport experiments were also analyzed using EPA Method 8515. The small size of the sand samples required a modification to the manufacturer's protocol. The test kit procedure calls for a 10 g soil sample, whereas we used a 1g sand sample. The ratio of sand to acetone/developer mix remained consistent with the manufacturer's instructions and the rest of the procedure was performed in general accordance with the protocol. Prior, to analysis, sand samples were air dried overnight in a 37^{o}C incubator. A stock of acetone/developer mix was made with a ratio of 50 mL of acetone to 2 drops of developer. Approximately 5 mL of the acetone/developer mix was added to 1 g of sand and shaken vigorously. Each sample was allowed a minimum of 10 minutes for the colorimetric reaction to occur before analysis. Then approximately 1 mL of liquid from each sample was extracted with a pipette and placed in a curvette. Samples were then processed with the spectrophotometer (A540).

EPA Method 8330

Effluent and sand samples from DNT experiments 4F, 5M and 6F were analyzed with the high-performance liquid chromatography based (HPLC) EPA Method 8330. HPLC is the EPA's recommended method for trace analysis of explosives residues in environmental samples. Numerous studies have demonstrated the effectiveness of the HPLC-based method for accurately detection of nitroorganic compounds (e.g. DNT, TNT, RDX, HMX) in soil and water, in particular at low concentrations in the sub ppb range (Bauer et al., 1986; Walsh et al., 1993; Guarvav et al., 2007). All 8330 analyses were performed by Accutest, a commercial lab in Orlando, Florida, in accordance with EPA guidelines (USEPA, 2009b). In this method, aqueous samples are diluted with acetonitrile, filtered and then separated on a C-18 reverse column. Analyte concentrations are determined at 254 nm wavelength with an ultraviolet detector and confirmed on a secondary CN reverse phase column (EPA, 2009b). Soil samples are extracted with acetonitrile in an ultrasonic bath and then processed in the same manner. For quality control purposes, analyses of each sample batch included a method blank, a blank spike, and matrix spike. Due to the small sample volumes, duplicates analyses were not performed.

Immunolabeling/Chemical Staining

Methods 8515 and 8330 were used to analyze the total concentration of DNT, both solid and dissolved, in effluent and sand samples. While the presence of particulate DNT in effluent samples can be inferred from the difference in concentrations in unfiltered and filtered samples, there is presently no method which can distinguish between solid and dissolved phase DNT in sand samples. Therefore, novel methods for the direct detection and quantitative analysis of particulate DNT in sand combining microscopy with the use of immunolabels and chemical stains were investigated.

Immunoassays were obtained from Strategic Diagnostics. The immunostaining technique uses commercial monoclonal antibodies directed against TNT (cross-reacting with 2,6- DNT) which have been fluorescently tagged with Oregon green. Non-specific binding was controlled using matched, fluorescently-tagged immunoglobulin control sera. Pure crystalline DNT was used to test the feasibility of immunolabeling and/or chemical staining of ER particles. Several DNT crystals (~50 mg total mass), with diameters of approximately 1 to 2 mm, were placed on a depression slide. Approximately 0.5 ml of the primary antibody solution, which bind with DNT, is applied to the crystals and allowed to sit for 30 minutes. Then, using a pipette, the solution is siphoned off and the crystals are flushed with approximately 1 mL water. The wash process is repeated three times after which 0.5 ml of the fluorescently tagged secondary antibody is applied and allowed to sit for 30 minutes. The secondary antibodies bind with the primary antibodies, thus labeling the DNT. The above described washing process is repeated after which microscopic image analysis is conducted.

Tetrabutylammonium hydroxide (TBAH) based chemical stain based was obtained from SACHEM. TBAH reacts with TNT to form a vivid red product. Taylor et al. (2004) reported the effective use of TBAH to identify TNT particles (>250 μm) collected from test detonations. Pure DNT powder, DNT mixed with loose Ottawa sand, and select sand samples from DNT column experiments were used to test the effectiveness of the TBAH stain.

First, various concentrations of TBAH mixed with water were applied to approximately 100 mg samples of pure DNT powder. The staining process was then observed over a period of 20 hours. Subsequently, TBAH, at the concentration previously determined to be most effective, was applied to both clean Ottawa sand samples (~250 mg) and sand samples mixed with approximately 100 mg of DNT. Depending on the results from the loose soil tests, TBAH was applied to select sand samples from particulate DNT transport experiments and imaged using transmitted-light brightfield microscopy.

Transport Modeling

Br- breakthrough data were used to characterize the transport of a non-reactive solute. This was accomplished by fitting the bromide data with a non-linear least-squares inversion modeling program, CXTFIT (Tang et al. 2010). The hydrodynamic dispersion coefficient (D) was determined using the advection-dispersion equation (ADE) (Van Genuchten and Alves, 1982):

$$\frac{\partial C}{\partial t} = -v\frac{\partial C}{\partial x} + D\frac{\partial^2 C}{\partial x^2}$$

Where C is the solute concentration (mg/l), x is distance (cm), v is the average pore water velocity (cm/s) (as determined by Darcy's Law), t is time (s), and D (cm^2/s) is defined as:

$$D = \alpha * v + D_e$$

Where α is dispersivity (cm) and D_e is the effective diffusion coefficient. Under rapid flow conditions diffusion is assumed to have minimal influence on hydrodynamic dispersion therefore was ignored for the purposes of these calculations.

Chapter 3: Results

DNT Particle Size Analysis

Results for the microscopy based particle size analyses of DNT powder batches (A, B, and C) are presented in **Figure 4**, as the percentage of the total number of particles counted per equivalent diameter size range. While not spherical, most of the particles observed were sub-rounded to sub-angular in shape so the equivalent diameter calculations should accurately estimate the size of the particles. The results indicate a good deal of variability of size distribution between batches, with a larger percentage of smaller particles observed in Batch A than in Batches B and C. This variability may have implications for the transport and persistence of the particles used in DNT particulate tracer experiments 1F-P and 2F-P (which used Batch A) versus 3F-P, 4F, and 5M (which used Batches B and C). However, for each batch the size distribution range falls between 35 um to < 2 um (the microscopy resolution limit was approximately 2 um), with the bulk of the particles (> 75% by number) being < 20 um in diameter at the start of each experiment.

Transport Experiments

Microsphere Tracer Experiments

Results for all microsphere tracer experiments (M1, M2, M3 and M4) are described in **Appendix B.**

DNT Particulate Tracer Experiments

Overview of DNT Experiments

One DNT tracer experiment (1F-P) was conducted with DNT particles suspended in the influent reservoir. A total of four DNT tracer experiments (2F-P, 3F-P, 4F, and 5M) were conducted with the DNT particles applied directly to the top sand layer of the columns. A final DNT tracer experiment (6F) was performed using dissolved DNT introduced from the influent reservoir.

Samples from preliminary experiments 1F-P, 2F-P, and 3F-P were analyzed at the University of Tennessee using method 8515. Samples from 4F and 5M were analyzed at Accutest Laboratories using method 8330. The preliminary experiments were conducted to establish simply whether DNT particulates could be transported and detected in effluent and sand samples. Method 8515, while not as quantitative as method 8330, was adequate for the purposes of these preliminary experiments.

Preliminary DNT Tracer Experiments - Method 8515 Analysis

DNT Particulate Suspension Experiment

Results for preliminary experiment 1F-P, with DNT particles suspended in the influent reservoir, are presented in **Figure 5a**. Values are plotted as DNT concentration in parts per million (ppm) for filtered and unfiltered samples as a function of pore volumes of effluent. For comparison purposes, bromide breakthrough data are also presented in **Figure 5a** as Br concentration in samples normalized to the influent concentration (C/C_o) versus effluent pore volume, illustrating the transport of a dissolved, non-reactive solute. In general, the unfiltered samples exhibit higher concentrations of DNT than the filtered aliquots, which would indicate DNT particles were present in the effluent. 1F-P breakthrough data are also presented in **Figure 5b** as cumulative DNT mass recovered for filtered and unfiltered samples normalized to the total mass of DNT input (M_e/M_o) versus effluent pore volume. Total DNT input mass was calculated using the influent concentration and the volume of influent solution applied to the column. Both filtered and unfiltered curves show a steady increase in cumulative mass recovered. Greater than 90% of the DNT recovered was in the unfiltered samples compared to approximately 60% recovered in the filtered samples, indicating a fraction of the DNT mass captured in the effluent was particulate. However, paired t-test statistical analysis of the data suggests there is no significant difference between the filtered and unfiltered samples at the 95% confidence level. No DNT was detected in the 1F-P sand samples analyzed using method 8515 (MDL 1 ppm). Mass balance calculations based on unfiltered effluent samples from 1F-P are presented in **Table 3**.

DNT Particulate Surface Application Experiment (preliminary)

Effluent results from the preliminary DNT particulate surface application experiment (2F-P) are presented in **Figure 6a**, with DNT concentration (ppm) for filtered and unfiltered samples plotted as a function of pore volume. Bromide data, plotted as Br concentration in samples normalized to the influent concentration (C/C_o) versus effluent pore volume, are also included in **Figure 6a**. Breakthrough data are somewhat scattered but generally level out at a concentration of approximately 5ppm. For some samples, the concentrations detected in the unfiltered aliquots are equal to or higher than the concentrations detected in the filtered sample aliquots, indicating the absence or presence of DNT particles respectively. However, there are also several instances in which the concentration detected in the filtered aliquot is higher than the concentration in the unfiltered aliquot. This suggests that concentration differences between the filtered and unfiltered samples falls within the standard error of the method 8515 analysis. Breakthrough data for unfiltered and filtered effluent samples from 2F-P are presented in **Figure 6b** as cumulative DNT mass recovered per pore volume normalized to the total mass of DNT applied to the surface of the column (Me/Mo). These data show an initial difference in mass recovered from filtered and unfiltered effluent, suggesting the presence of particulate DNT, but this separation converges as concentrations reach plateau values. Paired t-test statistical analyses of the filtered and unfiltered data from 2F-P suggest there is no significant difference between the two populations at the 95% confidence level.

Results for the distribution of the DNT in the sand from experiment 2F-P are presented in **Figure 7** as DNT concentration (μg/g) versus depth. Distribution of the DNT is exhibits a curvilinear decrease in concentration with depth. Mass balance calculations for 2F-P, summarized in **Table 3**, indicate relatively low total recovery.

Figure 8 compares normalized breakthrough curves of unfiltered and filtered samples from DNT particulate suspension experiment 1F-P and DNT particulate surface application tracer experiment 2F-P. The 1F-P data show a steeper breakthrough curve and a somewhat delayed arrival, relative to 2F-P. Both experiments show an initial difference in cumulative mass recovered in filtered versus unfiltered samples which tends to diminish as concentrations reach

the plateau values. However, in 1F-P, the separation in concentrations is slightly larger. In addition, 1F-P plateau concentrations indicate almost total mass recovery versus much lower mass recovery for 2F-P.

Main DNT Tracer Experiments - Method 8330 Analysis

DNT Particulate Surface Application Experiments

Two additional DNT particulate surface application experiments were conducted in fine (4F) and medium sand (5M). Samples from these experiments were analyzed at Accutest Laboratories using EPA method 8330. Results for unfiltered and filtered effluent samples from 4F and 5M are presented in **Figures 9a** and **9b**, respectively. Values are plotted as DNT concentration (ppm) versus pore volume of effluent. The unfiltered and filtered effluent aliquots for these two experiments show a definite separation in concentration. With the exception of one set of aliquots from 4F, concentrations for the unfiltered samples are equal to or higher than those for the filtered samples which implies the presence of particulate DNT. Paired t-test results suggest the difference between the filtered and unfiltered samples is highly significant ($p<0.01$) for 5M, but only marginally significant ($p = 0.06$) for 4F. Breakthrough data for unfiltered samples from 4F and 5M, presented as normalized cumulative DNT mass recovered versus pore volume of effluent (Me/Mo) versus depth (cm), is compared in **Figure 10**. The curves are virtually identical. **Figure 11** present the ratio of filtered to unfiltered DNT concentrations in samples from 4F and 5M versus effluent pore volume. Higher ratio values indicate a smaller difference in concentration between the filtered and unfiltered aliquots, therefore, less particulate DNT in the effluent. For most samples, the particulate DNT fraction accounts for approximately 20% more of the concentration in effluent from the medium sand experiment (5M) than it does for effluent from fine sand experiment (4F).

A comparison of the DNT distribution in the sand samples from experiments 4F and 5M is presented in **Figure 12**. Values are presented as DNT concentration (μg/g) versus depth (cm). As with the experiments 2F-P and 3F-P, sand samples from both columns exhibit a curvilinear

decrease in DNT concentration with depth. Nearly all of the DNT mass is in the top two centimeters of sand, indicating only a small fraction has been transported further. DNT concentrations throughout the lower half of the column are somewhat higher for 4F sand samples.

Mass balance results for 4F and 5M are summarized in **Table 3**. Mass balance calculations for the effluent indicate a slightly higher percentage of DNT mass recovered in the effluent of the fine column (~ 9 %) than that of the medium column (~ 7 %). However, based on concentration differences between the filtered and unfiltered aliquots, particulate DNT accounts for approximately 30 % of the DNT mass recovered in the effluent of the medium sand column versus less than 15 % of the mass recovered in the effluent from fine sand column. Overall mass balance results for the sand samples are similar for both sand types.

Comparison of analytical methods 8515 and 8330

Due to the multiple incidences in which method 8515 analytical results showed DNT concentrations in filtered samples were higher than those in the unfiltered aliquots, an additional DNT particulate surface application experiment (3F-P) was conducted to test the reproducibility of this method. The data are presented in **Figure 13** which compares the DNT concentrations detected in duplicate filtered and unfiltered effluent samples. The results indicate a very low level of reproducibility.

Effluent results for 2F-P, analyzed at the University of Tennessee using method 8515, are quite different than those for 4F and 5M, analyzed at Accutest Laboratories using method 8330.A comparison of the normalized cumulative mass recovered (M_e/M_o) in unfiltered effluent samples from DNT particulate surface application experiments (2F-P, 3F-P, 4F, and 5M) is presented in **Figure 14**. Although experimental conditions and the total mass of DNT particulate applied were similar for all four experiments, 4F and 5M exhibit significantly higher breakthrough concentrations. A comparison of the normalized cumulative mass recovered (M_s/M_o) in sand samples DNT particulate surface application experiments (2F-P, 4F, and 5M) are presented in **Figure 15.** The sand curves all are strikingly similar in shape but as with the effluent curves, the

concentration of DNT in samples from 2F-P is lower than those of 4F and 5M. Overall, mass balance results for experiments 4F and 5M were much better. This, coupled with the poor reproducibility indicated by the results for the effluent sample duplicates from experiment 3F-P, suggests the 8515 analytical method is inaccurate.

To test whether the two analytical methods were producing different results, additional unfiltered effluent samples from 4F were processed at using method 8515. The selected samples represent the unfiltered effluent aliquots from pore volumes which fall between previously produced unfiltered breakthrough data points from the 8330 analysis. A comparison of results from the original samples analyzed using method 8330 to the results from samples subsequently analyzed using method 8515 analysis is presented in **Figure 16**. Values are plotted as DNT concentration (ppm) from unfiltered samples versus pore volume of effluent. Results from the samples analyzed using method 8330 indicate concentrations of approximately 100 ppm, with the exception of the sample from earliest pore volume analyzed. However, results for all samples analyzed using method 8515 indicate DNT concentrations below the minimum detection limit of the test kit (reported by manufacturer as 1 ppm).

Dissolved-phase DNT experiment

Results for the dissolved-phase DNT experiment (6F) are presented in **Figure 17**, as DNT concentration detected in samples normalized to the concentration in the influent reservoir (C/Co) versus pore volume of effluent. The breakthrough curve has an irregular shape and normalized DNT concentrations never exceed 60% of the input concentration. Results for the sand samples are presented in **Figure 18**, as DNT concentration (ug/g) versus depth (cm). DNT distribution in the sand is variable in the upper and lower sections the column, with concentrations ranging from approximately 0.6 ug/g to close to the minimum analytical detection limit of 0.06 ug/g. Concentrations in the middle of the column (from 4 to12 cm depth) are below the MDL. Overall, mass balance results for 6F are low with only 45.5% of the total mass of DNT recovered (see **Table 3**).

Figure 19 compares the effluent results for from 6F to results for filtered samples from DNT particulate surface application experiment 4F. Values are presented as cumulative DNT mass

recovered in samples normalized to the total mass of DNT applied to the column versus pore volume of effluent. In 6F, the DNT arrival time is slightly delayed, relative to 4F, and it takes more than three pore volumes to achieve plateau concentrations. The total percent of DNT mass recovery in the effluent samples from 4F is approximately an order of magnitude lower than 6F.

Bromide Tracer and Modeling Results

Bromide tracers and modeling results are presented in **Appendix C**.

Detection Method Development

Immunolabeling

Fluorescently labeled antibodies were applied to a crystalline DNT sample which was subsequently imaged with a confocal microscope equipped to detect the correct wavelength. However, no fluorescently tagged DNT particles were observed.

Chemical staining

Figure 20 presents images of pure DNT powder reacting with different concentrations of TBAH (6.9% to 55% TBAH in water) over a period of 20 hours. At the highest TBAH concentration, the reaction is instantaneous but tends to dissolve the DNT particles quickly. At the low concentrations, the reaction is slow (> 20 hours), producing only a weak color change. For the purposes of detecting and imaging DNT particles in the micron size range, TBAH concentration of 15 to 30% was optimal.

The application of TBAH to loose Ottawa sand mixed with DNT and to select sand samples from transport experiments also proved effective for qualitatively identifying particulate DNT. **Figure 21** presents images of a sand sample before and after treatment with TBAH (sand from DNT surface application experiment 2F-P, collected 3 cm below top of column). It was possible to detect TBAH-stained particles > 50 um diameter using brightfield microscopy, however a

significant degree of dissolution of DNT particles was observed within the 5 minutes between the reaction start and the time the image was captured. Intact particles < 50 μm were not observable, although point sources of diffused red-colored product suggest that smaller DNT particles may have been present but were completely dissolved by the TBAH reaction.

Chapter 4: Discussion

Development of Experimental Methods

Before conducting the main transport experiments it was necessary to establish methods: to produce a surrogate for fine-grained ER particles, quantify the size distribution of the ER particulate surrogate, and apply the ER particulate surrogate to the column set-up. In addition, it was desirable to develop detection techniques that could identify and quantify the presence of ER particulate surrogate in sediments. Details regarding which methods were more or less effective are presented in this section, as well as discussion of the main experimental outcomes.

DNT particle size and flocculation

Each of the three batches of DNT powder were comprised of a relatively wide size range of particles (<2 to >36 μm). Only a small fraction of the particles were in the size range which likely to be mobile in the granular media used in these experiments (<2 um). Considering size exclusion alone, it can be hypothesized that the smaller DNT particles are mobile at the beginning of the experiment while the larger particles remain immobile until their size is reduced by dissolution. The percentage of particles in this potentially mobile size range varied from batch to batch of DNT powder. Thus, the number of potentially mobile DNT particles initially applied to the different columns was not consistent. The size distribution would also affect the rate at which the DNT particles dissolve. Smaller particles have a higher surface area to mass ratio, and can thereby dissolve faster. In effect, the DNT batches with a greater percentage of small particles could potentially produce additional "mobile size range" particles and dissolved-phase DNT more quickly than batches consisting of a higher percentage of larger particles. Therefore, this variability in particle size distribution from batch to batch has implications for the transport experiments. However, no clear effects were observed in the experimental outcomes.

Microscopic analysis of the powder batches revealed that the DNT particles have a tendency to flocculate when immersed in water. This could be a hydrophobic interaction caused by the

aromatic ring structure of DNT (Reusch, 2010). Also, stacking due to π-π interactions is of particular importance to the intermolecular interactions of heterocyclic aromatics and could encourage the aggregation of the particles (Choudhury & Chitra, 2010). Alternately, the flocculation may be related to excess surface energy imparted to the particles by mechanochemical effects from the grinding process (Masuda et al., 2007). The addition of a 1% solution of bovine serum albumin (BSA) surfactant to the water/DNT powder mixture was effective in dispersing the particles for microscopic imaging. However, even with BSA, DNT particle aggregates still formed in the influent solution used for experiment 1F-P (**Figure 22**). It is also possible that the use of the surfactant influenced the transport of the particles in the column.

Methods for Detecting DNT

Labeling particulate DNT

Efforts to develop a quantitative detection method for particulate DNT using immunoassays and chemical stains with microscopic image analysis were unsuccessful. In all cases, the solubility of DNT was the issue. The immunolabeling process appears to cause the partial dissolution of the particulate DNT, resulting in the cognate antibodies binding with the dissolved-phase before coming into contact with the solid-phase DNT. The antibodies are subsequently removed in the washing processes, leaving only the unlabeled particulate DNT behind.

Like immunolabeling, the chemical staining process also causes the DNT particulate to dissolve. The use of TBAH was effective for the qualitative identification of larger DNT particles (>50 um). However, smaller particles (<20um) are dissolved too fast for image analysis to be performed. The speed of the colorimetric reaction is dependent on the concentration of TBAH. Higher concentrations of TBAH lead to a faster staining process but also appear to dissolve the DNT more quickly. Conversely, a lower concentration of the of TBAH would dissolve DNT more slowly but also cause the staining process to take longer, hence giving the DNT more time to dissolve.

Comparison of analytical methods 8515 and 8330

Preliminary DNT tracer experiments M1, 2F-P, and 3F-P were analyzed with colorimetric-based EPA method 8515 at the University of Tennessee while later DNT tracer experiments (4F, 5M and 6F) were analyzed by HPLC-based EPA method 8330. A comparison of results produced by the different analytical techniques clearly indicates there are problems with the accuracy and precision of the 8515 method. A possible source of error is our modification of the test kit protocol. Good results for the stock solutions (1, 5, 15, 30 ppm) used for calibration of the spectrophotometer suggest the test kit developer functioned properly. However, the calibration solutions were created by mixing DNT directly with reagent grade acetone, precluding the inclusion of any water which could inhibit the colorimetric reaction. On the other hand, for the effluent samples, the DNT must be removed from the water for analysis. The manufacturers' protocol calls for the use of an extraction filter and vacuum filtration system to sequester the DNT and remove excess water. The use of a vacuum centrifuge instead of the filtration process could have led to sample loss or the incomplete removal of water from the effluent samples. Sample loss could occur if the centrifuge was unbalanced or if the vacuum improperly applied, resulting in the lower effluent concentrations. Regarding the question of excess water, Dimitriu et al. (2009) observed that the TBAH colorimetric reaction is sensitive to the addition or absence of solvents other than the proscribed methanol or acetone. In a study examining similar alkaline reagents used to identify nitroaromatic compounds in soils, Jenkins and Walsh (1992) noted that in the case of 2,4-DNT too little, or conversely too much, water inhibits the colorimetric reaction. They concluded that for the detection of DNT in soils the optimal moisture content range was small, from 1-10% (wet weight basis). This could explain why the DNT concentrations from the sand samples analyzed with 8515 analysis were also lower than expected, as they were air dried in a 37^{o}C incubator perhaps resulting in a moisture content <1%.

It is most likely that method 8515, which is generally used for screening soil for the presence or absence of explosives rather than quantitative analysis, simply lacks the accuracy required for the purposes of this study. Given the questionable reliability of this adapted 8515 method, the accuracy of the data from experiments 1F-P, 2F-P and 3F-P is uncertain. In general, the 8515

method appears to underestimate the actual DNT concentrations in samples. Nonetheless, the overall trends of DNT breakthrough in the effluent and spatial distribution in the sand are similar to those from experiments processed by method 8330.

DNT Tracer Experiments

Dissolved phase experiment

The breakthrough curve for 6F suggests that the DNT may be adsorbing to the sand. However, very little DNT was detected in the column sand. Overall, the total mass recovery results from this experiment are significantly lower than those of other experiments analyzed with the 8330 method. This suggests that some of the DNT may have sorbed to experimental set-up material, most likely the tubing from the influent reservoir. Therefore, the usefulness of any interpretation based on the 6F dataset would be very limited.

This possible sorption to the experimental set-up materials may also have implications for the particulate suspension DNT experiment (1F-P) in which the DNT was also introduced from the influent reservoir. Mass recovery results for experiment 1F-P are good, but the total DNT mass input to the column is poorly constrained due to the heterogeneous distribution of particulate DNT suspended in the reservoir. It is possible that more DNT was actually input to the column than is indicated by calculations based on the analytical results of the influent samples and that in reality the mass recovery percentages are lower.

DNT Suspension Experiment

The input of particulate DNT suspended in an influent solution does not appear to be a feasible technique for column transport experiments. Even with the addition of BSA, the formation of aggregates prevents the homogenous distribution of the DNT particles in the influent water and hinders the movement of these materials from the reservoir to the column. The persistence of the particulate aggregates also provides anecdotal evidence of a relatively slow DNT dissolution

rate. This is supported by the analytical results for the influent concentration. Although 300 mg of DNT was added to 1 L of influent solution and the solubility of DNT at room temperature is reportedly ~200 mg/L, the post experiment dissolved DNT concentration in the reservoir was only < 2 mg/L. Alternatively, since the samples from experiment M1 were processed with method 8515, the analytical results may underestimate the influent concentration.

Interpretation of the experimental results is also complicated by a poorly constrained DNT input mass, both in the dissolved and solid phase. Influent samples were collected directly from the reservoir, after the completion of the transport experiment. Although the time frame of the experiment was short (approximately 40 minutes), dissolved DNT input concentrations may have been lower at the beginning. Also, since the distribution of the DNT particles in the influent solution was not homogenous, it was not possible ascertain the total DNT mass applied to the column or what fraction of that mass was particulate material.

Concentration differences between the filtered and unfiltered influent samples are small (~ 0.3 ppm). This suggests that the mass fraction of dispersed DNT particulate material was insignificant, with the bulk of particles trapped in aggregates floating on the surface of the reservoir solution. Like the dissolved-phase input concentration, it is possible that the amount of solid-phase DNT applied to the column may have varied over the course of the experiment. However, the high percentage of total mass recovered suggests that the influent sample concentrations were reasonably representative.

Results for 1F-P indicate that particulate material did not account for a statistically significant portion of the DNT mass recovered in effluent samples. Furthermore, no DNT was detected in sand samples from 1F-P, indicating the DNT in the column material had been completely eluted by the background solution washout or the residual concentrations were below analytical detection limits of method 8515. This is further evidence that most of the particulate material remained trapped in the reservoir. If a sizable mass had been applied to the column it is likely that a portion of it would have been retained in the sand at detectable levels.

Particulate DNT surface application experiments

The application of solid-phase material to the top of the column pack proved to be an effective method for introducing DNT particulate material to the experimental system. This method allows for an accurate measurement of the total DNT mass applied and more accurately represents field conditions than introduction of the material as a suspension.

In each surface application experiment transport of the DNT occurred in both the solid and dissolved phase. Dissolved phase transport of the DNT was limited in part due to the ratio of solid phase DNT mass applied to a column (>300 mg) to the volume of influent solution available to dissolve it (< 150 mL). Based on a consideration of solubility alone, only approximately 10% of the solid DNT phase could have dissolved. However, mass recovery results for the filtered effluent samples were typically closer to 1%. In a clean acid washed sand free of organic material sorption of an organic compound such as DNT is unlikely. This suggests that dissolved phase transport was also constrained by a slow dissolution rate.

In all cases, most of the DNT mass is retained in the column sand with only a small fraction recovered in the effluent. This curvilinear decrease in concentration with depth has also been observed in other experimental studies using microspheres (Bradford et al., 2002, Johnson et al., 2007). A slow dissolution rate would also inhibit the particulate transport of DNT, as only a small percentage of the DNT particles applied to column were initially within a size range expected to be mobile (<5 μm diameter). However, the spatial distribution of DNT in the sand from each surface application experiment does suggests that a significant portion of the particulate DNT mass is migrating through at least the top half of the column.

The translocation of particulate DNT deeper within the column would enhance dissolved phase breakthrough. Even if a particle is retained in the sand, the distance between a portion of the DNT source, albeit small, and the effluent collection point has been effectively reduced, thereby shortening the time it takes for the dissolved phase DNT to reach the bottom of the column. The presence of particulate DNT in effluent samples, as inferred from the difference between filtered

and unfiltered sample concentrations, was detected in each surface application experiment. However, the inferred particle mass was a small fraction of the total DNT mass of recovered in the effluent. The separation between the filtered and unfiltered aliquots was only statistically significant for the experiment conducted in the medium sand (5M). This suggests a larger amount, and/or size, of DNT particles could be transported in a coarser grained medium or in soils containing macropores.

Similar observations have been made in other studies of colloidal transport. Both Bradford et al. (2002) and Knappet et al., (2009) observed a positive relationship between increased grain size and peak effluent concentrations for column experiments conducted with microspheres in granular porous media. Likewise, studies investigating the transport of microorganisms, such as *C. Parvum,* in sandy aquifers have shown decreased retention with increased median grain size (Kim et al., 2010).

Very few transport experiments have been conducted using particulate explosives materials. Dontsova et al. (2006) and Dontsova et al. (2009) performed transport experiments using CB residues from low order detonations and DNT from MI propellant, respectively, which were applied to column materials in a fashion similar to this study. However, these studies assumed that dissolution of the particulate ER material occurred on the top surface of the column and subsequent transport was in the dissolved phase. Effluent samples were not analyzed for the presence of particulate material (e.g. using filtered aliquots) therefore it can't be determined whether solid phase transport of ER occurred in these experiments as well.

Chapter 5: Conclusions & Recommendations

Methods for the direct detection of particulate explosives residues

Due to the solubility of DNT, immunolabeling and chemical staining are not effective methods for the quantitative analysis of microscopic particles. It is probable, that the same issue will also hinder the use of these techniques for identifying micron size ER particles. This study also shows that the colorimetric-based method 8515, while useful for screening (presence/absence) for particulate ER surrogate in sediments, is not quantitative.

The development of a detection method that can differentiate between particulate and dissolved phase ER material in soils would greatly assist future research and understanding of ER transport. It may be possible to label less soluble TNT, RDX and HMX particles using immunolabeling and/or chemical staining. Further tests conducted with these compounds are required to determine whether these are viable methods for the detection of actual explosives residues.

Transport of particulate explosives residues

The DNT particulate tracer experiments show that the transport of DNT particles through saturated porous media is possible. Transport of an explosives residues surrogate through granular porous media occurs in both the solid and dissolved phase. It is likely that fine ER particles could be transported through vadose soils under saturated conditions. Under these experimental conditions (i.e., homogeneous porous media), DNT particulate did not account for a very significant fraction of the total mass recovered in the effluent. However, the transport of particulate DNT might be enhanced by the presence of macropores found in many soil types. In material with characteristics ideal for colloidal transport, the transport of particulate ER could contribute to the contamination of aquifers underlying these ranges. Transport experiments using particulate DNT in media with larger pore structures, such as large glass beads, would provide greater insight to the influence of macropores on ER transport. Further research is required to

determine if actual explosives residues (TNT, RDX, HMX) exhibit the same potential for transport as the ER surrogate used in this study. In addition, more realistic experiments using intact soil columns are needed to investigate the effects of natural structures and geochemical properties on the movement of particulate ER.

References

Agency for Toxic Substances and Disease Registry (ATSDR) 2010, Center for Disease Control, Atlanta, GA, viewed 29 June, 2010, < http://www.atsdr.cdc.gov/ >.

Becker, MW, Reimus, PW, & Vilks, P 1999, 'Transport and attenuation of carboxylate-modified latex microspheres in fractured rock laboratory and field tracer tests', *Ground Water*, vol. 37, no. 3, pp. 387-395.

Bauer, CF, Grant, CL, & Jenkins, TF 1986, 'Interlaboratory evaluation of high-performance liquid chromatographic determination of nitroorganics in munition plant wastewater', *Anal. Chem.*, vol. 58, pp. 176-182

Bradford, SA & Bettahar, M 2006, 'Significance of straining in colloid deposition: Evidence and implications', *Water Resour. Res.*, vol. 42, pp. 1-16.

Bradford, SA, Yates, SR, Bettahar, M & Simunek, J 2002, 'Physical factors affecting the transport and fate of colloids in saturated porous media', *Water Resour. Res.*, vol. 38, pp. 1-12

Cey, EE, Rudolph, DL, & Passmore, J 2009, 'Influence of macroporousity on preferential solute and colloid transport in unsaturated field soils', *J. Contam. Hydrol.*, vol. 107, pp. 54-57.

Choudhury, RR & Chitra, R 2010, 'Stacking interaction between homostacks of simple aromatics and the factors influencing these interactions' *CrystEngComm*, vol. 12, pp. 2113-2121.

Clausen, JL, Korte, N, Dodson, M, Robb, J & Rieven, S 2006, *Conceptual model for the transport of energetic residues from surface soil to groundwater by range activities*, ERDC/CRREL TR-06-18, US Army Engineer Research & Development Center, Hanover, NH.

Cumbie, DH & McKay, LD 1999, 'Influence of particle diameter on particle transport in a fractured shale saprolite', *J. Contam. Hydrol.*, vol. 37, pp. 139-157.

DeNovio, NM, Saiers, JE, & Ryan, JN 2004, 'Colloid movement in unsaturated porous media: Recent advances and future directions', *Vadose Zone J.*, vol. 3, pp. 338-351.

Dimitriu, E, Moldoveanu, SC, Iorgulescu, EE 2009, 'Solvent-Reagent effect in chemical detection of energetic materials type contaminants', *Russ. J. Phys. Chem.*, vol. 83, pp. 1537-1541.

Dontsova, KM, Pennington, JC, Hayes, C, Simunek, J, & Williford, CW 2009, 'Dissolution and transport of 2,4-DNT and 2,6-DNT from M1 propellent in soil columns'Chemosphere, vol. 77, pp. 597-603.

Dontsova, KM, Yost, SL, Simunek, J, Pennington, JC & Williford, CW 2006, 'Dissolution and transport of TNT, RDX, and Composition B in saturated soil columns' *J. Environ. Qual.*, vol. 35, pp. 2043-2054.

El-Farhan, YH, DeNovio, NM, Herman, JS, & Hornberger, GM, 2000, 'Mobilization and transport of soil particles during infiltration experiments in an agricultural field, Shenandoah Valley, Virginia', *Environ. Sci. Technol.*, vol. 34, no. 17. Pp. 3555–3559.

Elgrabli, D, Abella-Gallart, S, Aguerre-Chariol, O, Robidel, F, Rogeriuex, F, Boczkowski, J, & Lacroix, G 2007, 'The effect of BSA on carbon nanotube dispersion for *en vivo* and *in vitro* studies', *Nanotoxicology*, vol. 1, no. 4, pp. 266-278.

Fetter, CW 1994, *Applied Hydrogeology*, 3rd edn, Prentice Hall, Upper Saddle River, NJ.

Gaurav, D, Malik, AK & Rai, PK 2007, 'High-Performance Liquid Chromatographic Methods for the Analysis of Explosives', *Crit. Rev. Anal. Chem.*, vol. 37, no. 4, pp. 227-268.

Hewitt, AD, Jenkins, TF, Ramsey, CA, Bjella, KL, Ranney, TA, & Perron NM 2005, *Estimating energetic residue loading on military artillery ranges*, ERDC/CRREL report TR-05-7, US Army Engineer Research & Development Center, Hanover, NH.

Jenkins, TF, Hewitt, AD, Grant, CL, Thiboutot, S, Ampleman, G, Walsh, ME, Ranney, TA, Ramsey, CA, Palazzo, AJ, & Pennington, JC 2006, 'Identity and distribution of residues of energetic compounds at army live-fire training ranges', *Chemosphere*, vol. 63, pp. 1280-1290.

Jenkins, TF, Pennington, JC, Ranney, TA, Berry, TE, Miyares, PH, Walsh, ME, Hewitt, AD, Perron, NM, Parker, LV, Hayes, CA, & Wahlgren, EG 2001, *Characterization of explosives contamination at military firing ranges*, ERDC/CRREL report TR-01-5, US Army Engineer Research & Development Center, Hanover, NH.

Jenkins, TF, Walsh, ME, Thorne, PG, Miyares, PH, Ranney, TA, Grant, CL & Esparza, JR 1998, *Site characterization for explosives contamination at a military firing range impact area*, Special Report 98-9, US Army Engineer Research & Development Center, Hanover, NH.

Jenkins, TF & Walsh, ME 1992, 'Development of filed screening methods for TNT, 2,4-DNT and RDX in soil', *Talanta*, vol. 39, no. 4, pp. 419-428.

Johnson, WP, Li, X, & Assemi, S, 2007, 'Deposition and re-entrainment dynamics of microbes and non-biological colloids during non-perturbed transport in porous media in the presence of an energy barrier to deposition', *Adv. Water Resour.*, vol. 30, pp, 1432-1454.

Kim HN, Walker, SL, & Bradford, SA 2010, 'Coupled factors influencing the transport and retention of Cryptosporidium parvum oocysts in saturated porous media', *Water Res.*, vol. 44, pp. 1213-1223.

Knappett, PSK, Emelko, MB, Zhuang, J, & McKay, LD 2008, 'Transport and retention of a bacteriophage and microspheres in saturated, angular porous media: Effects of ionic strength and grain size', *Water Res.*, vol. 42, pp. 4368-4378.

Lindqvist, R & Bengtsson, G 1995 'Diffusion-limited and chemical-interaction-dependent sorption of soil bacteria and microspheres' *Soil Biol. Biochem.*, vol. 21, no. 1, pp. 941-948.

Luning Prak, DJ, O'Sullivan, DW 2007, 'Solubility of 4-Nitrotoluene, 2,6-Dinitrotoluene, 2,3-Dinitrotoluene, and 1,3,5-Trinitrobenzene in pure water and seawater', *J. Chem. Eng. Data*, vol. 52, pp. 2446-2450.

Masuda, H, Higashitani, K, & Yoshida, H (eds) 2007, *Powder Technology: Fundamentals of particles, powder beds, and particle generation*. CRC press, New York, NY.

McCarthy, JF & McKay, L D 2004, 'Colloid transport in the subsurface: Past, present, and future challenges', *Vadose Zone J.*, vol. 3, pp. 326-337.

McCarthy, JF & Shevenell, L. 1998, 'Processes controlling colloid composition in a fractured and karstic aquifer in eastern Tennessee, USA', *J. Hydrol.*, vol. 206, pp. 191-218.

McCarthy, JF & Zachara, JM 1989, 'Subsurface transport of contaminants: Mobile colloids in the subsurface environment may alter the transport of contaminants' *J. Environ. Sci. Technol.*, vol. 23, no. 5, pp. 496-502.

Military.com 2010, Military Advantage, San Francisco, CA, viewed 29 June, 2010, <http://www.military.com/>.

Morley, MC, Yamamoto, H, Speitel, GE & Clausen, J 2006, 'Dissolution kinetics of high explosives particles in a saturated sandy soil', *J. Contam. Hydrol.*, vol. 85, pp. 141-158.

Pennington, JC, Thorn, KA, Hayes, CA, Porter, BE, & Kennedy, KR 2003, 'Immobilization of 2,4- and 2,6-Dinitrotoulene in soils and compost', ERDC/CRREL report TR-03-2, US Army Engineer Research & Development Center, Hanover, NH.

Poulsen, TG, Moldrup, P, de Jonge, LW & Komatso, T 2006, 'Colloid and bromide transport in undisturbed soil columns: Application of two-region model', *Vadose Zone J.*, vol. 5, pp. 649-656.

Reusch, WH 2010, *Virtual Textbook of Organic Chemistry*, viewed 9 September, 2010, <http://www2.chemistry.msu.edu/faculty/reusch/VirtTxtJml/intro1.htm>.

Ryan, JN, Illangasekare, TH, Litaor, MI, & Shannon, R 2008, 'Particle and Plutonium mobilization in macroporous soils during rainfall simulations', *J. Environ. Sci. Technol.*, vol. 32, pp. 476-482.

Shang, J, Flury, M, Chen, G, Zhuang, J 2008, 'Impact of flow rate, water content, and capillary forces on in situ colloid mobilization during infiltration in unsaturated sediments', *Water Resour. Res.*, vol. 44, pp.

Sirivithayapakorn, S & Keller, A 2003, 'Transport of colloids in unsaturated porous media: A pore-scale observation of processes during dissolution of air-water interface', *Water Resour. Res.*, vol. 39, no. 12, pp. 1346-1356.

Snyder, LR & Kirkland, JJ 1979, *Introduction to Modern Liquid Chromotography*, Wiley, New York, NY.

Suttiprasit, P, Krishdhasima, V, & McGuire J 1992, 'The surface activity of α-lactalbumin, β-lactoglobulin, and bovine serum albumin: Surface tension measurements with single-component and mixed solutions'. *J. Colloid Interface Sci.*, vol. 154, pp. 316-326.

Tang, G, Mayes, MA, Parker, JC, & Jardine, PM 2010, 'CXTFIT/Excel – A modular adaptable code for parameter estimation, sensitivity analysis and uncertainty analysis for laboratory or field tracer experiments'. *Computers & Geosciences*, vol. 36, pg 1200-1209.

Taylor, S, Campbell, E, Perovich, L. Lever, J & Pennington, J 2006, 'Characteristics of Composition B particles from blow-in-place detonations', *Chemosphere*, vol. 65, pp. 1405-1413.

Taylor, S, Hewitt, A, Lever, J, Hayes, C, Perovich, L, Thorne, P & Daughlian, C 2004, 'Particle size distribution from detonated 155-mm howitzer rounds' *Chemosphere*, vol. 55, pp. 357-367.

Thiboutot, S, Ampleman, G, Gagnon, A, Marois, A, Jenkins, TF, Walsh, ME, Thorne, PG & Ranney TA 1998, *Characterization of anti-tank firing ranges at CFB Valcartier, WATC Wainwright and CFAD Dundurn*, Report # DREV-R-9809, Defense Research Establishment, Val-Belair, Quebec.

U.S. Environmental Protection Agency 2009a, *Drinking Water Standards and Health Advisories*, EPA 822-R-09-011, U.S. Environmental Protection Agency, Washington, DC.

U.S. Environmental Protection Agency 2009b, *Test Methods for Evaluating Solid Waste, Physical/Chemical Methods (SW-846)*, U.S. Environmental Protection Agency, Washington, DC., viewed 12 July, 2010, <http://www.epa.gov/osw/hazard/testmethods/sw846/online/index.htm >.

Van Genuchten, MT & Alves, WJ 1982, *Analytical Solutions of the One-Dimensional Convective-Dispersive Solute Transport Equation.* United States Department of Agriculture, Agricultural Research Service, Technical Bulletin 1661.

Vesper, DJ & White, WB 2003, 'Metal transport to karst springs during storm flow: an example from Fort Campbell, Kentucky/Tennessee, USA', *J. Hydrol.*, vol. 276. pp. 20-36.

Walsh, ME, Jenkins, TF, Schnitker, PS, Elwell, JW & Stutz, MH 1993, 'Evaluation of SW846 method 8330 for characterization of sites contaminated with residues of high explosives', CRREL report 93-5, US Army Engineer Research & Development Center, Hanover, NH.

Wan, J & Tokunaga, TK, 1997, ‘Film straining of colloids in unsaturated porous media: Conceptual model and experimental testing’, *J. Environ. Sci. Technol.*, vol. 31, pp. 2413-2420.

Zhuang, J, Tyner, JS & Perfect, E 2009, ‘Colloid transport and remobilization in porous media during infiltration and drainage’, *J. Hydrol.*, vol. 377, pp. 112-119.

Zvikelsky, O & Weisbrod, N 2006, ‘Impact of particle size on colloid transport in discrete fractures’, *Water Resour. Res.* Vol. 42, W12S08, doi:10.1029/2006WR004873

Appendix A

Figures

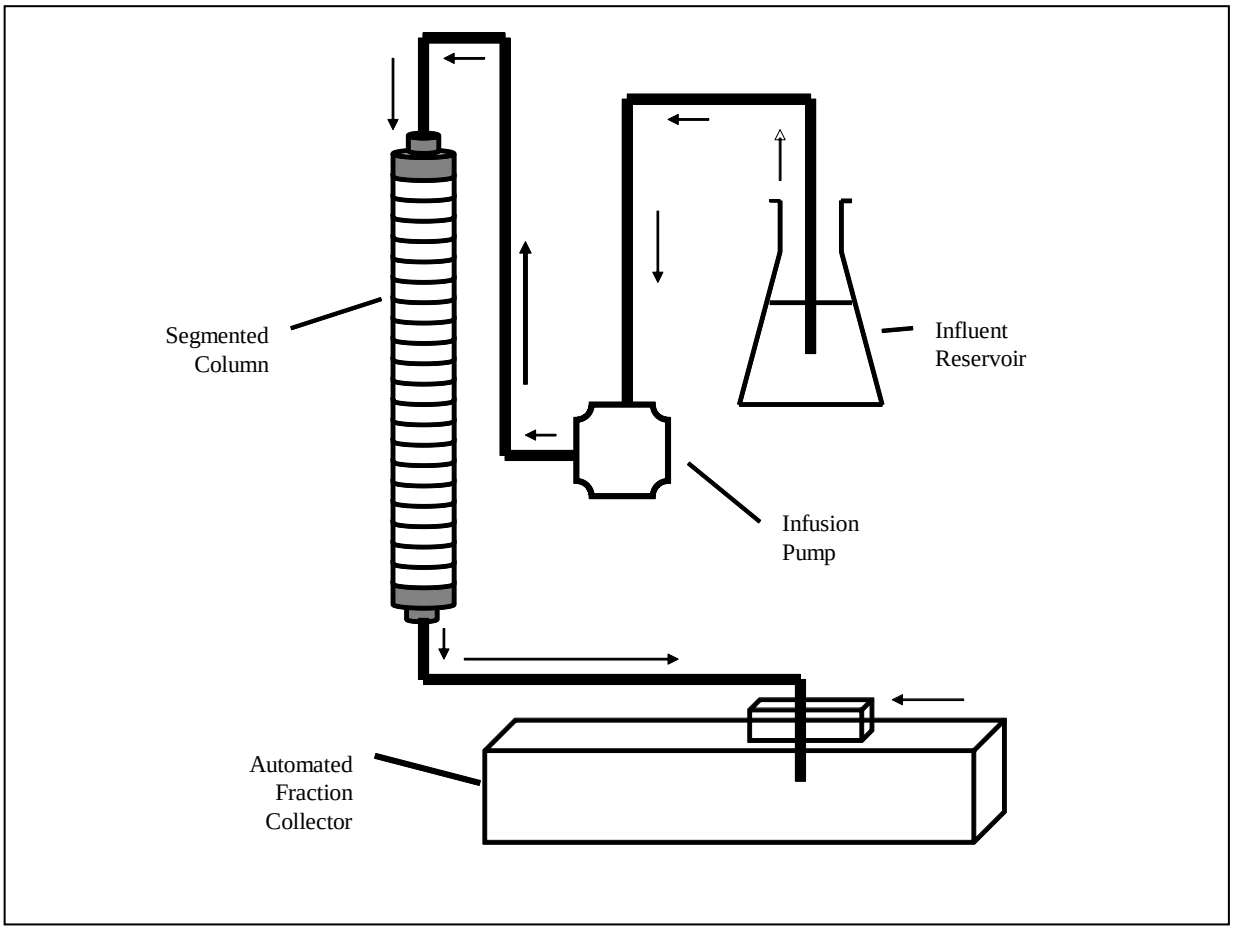
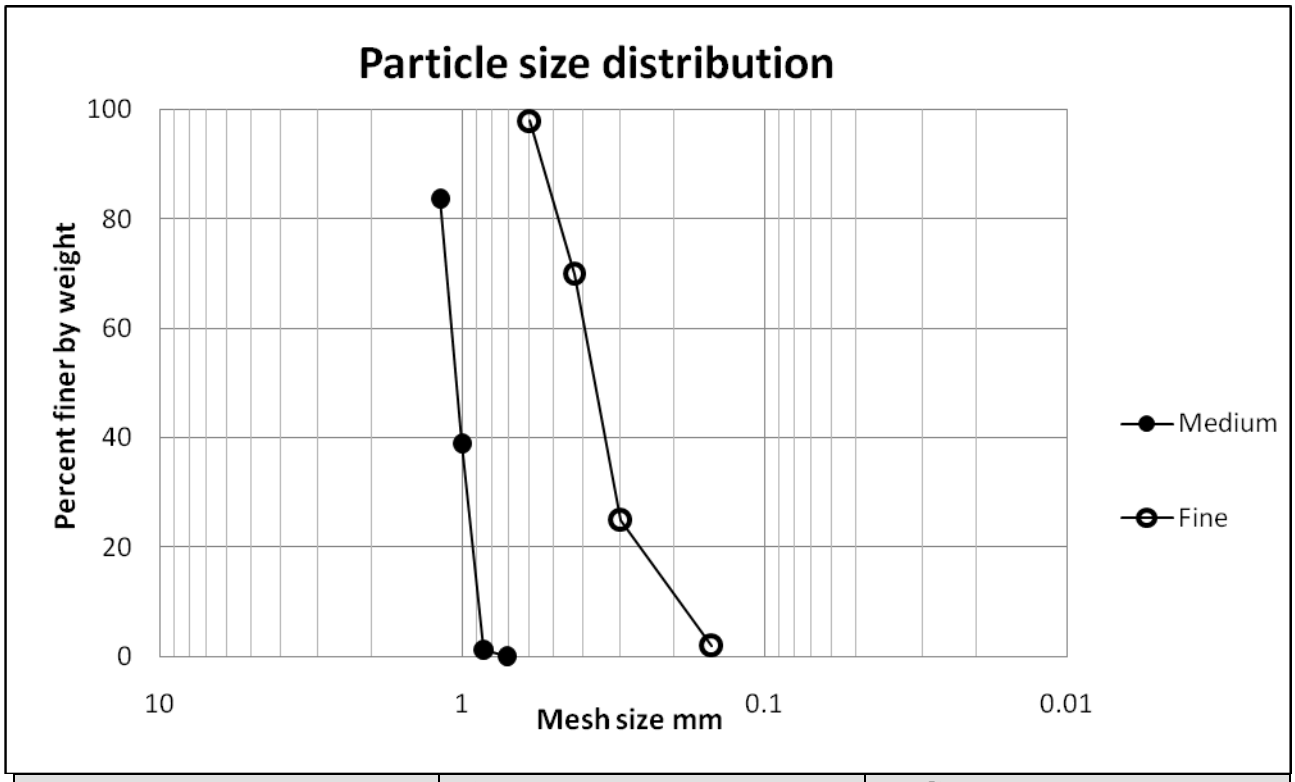


Figure 1- Experimental set-up



	Fine	Medium
d_{10}	0.196 mm	0.823 mm
d_{50}	0.374 mm	1.04 mm
d_{60}	0.419 mm	1.09 mm
Uniformity Coefficient	2.14	1.32

Figure 2 – Particle size distribution
Particle size distribution for the fine and medium Ottawa sands (based on distributor's specifications).

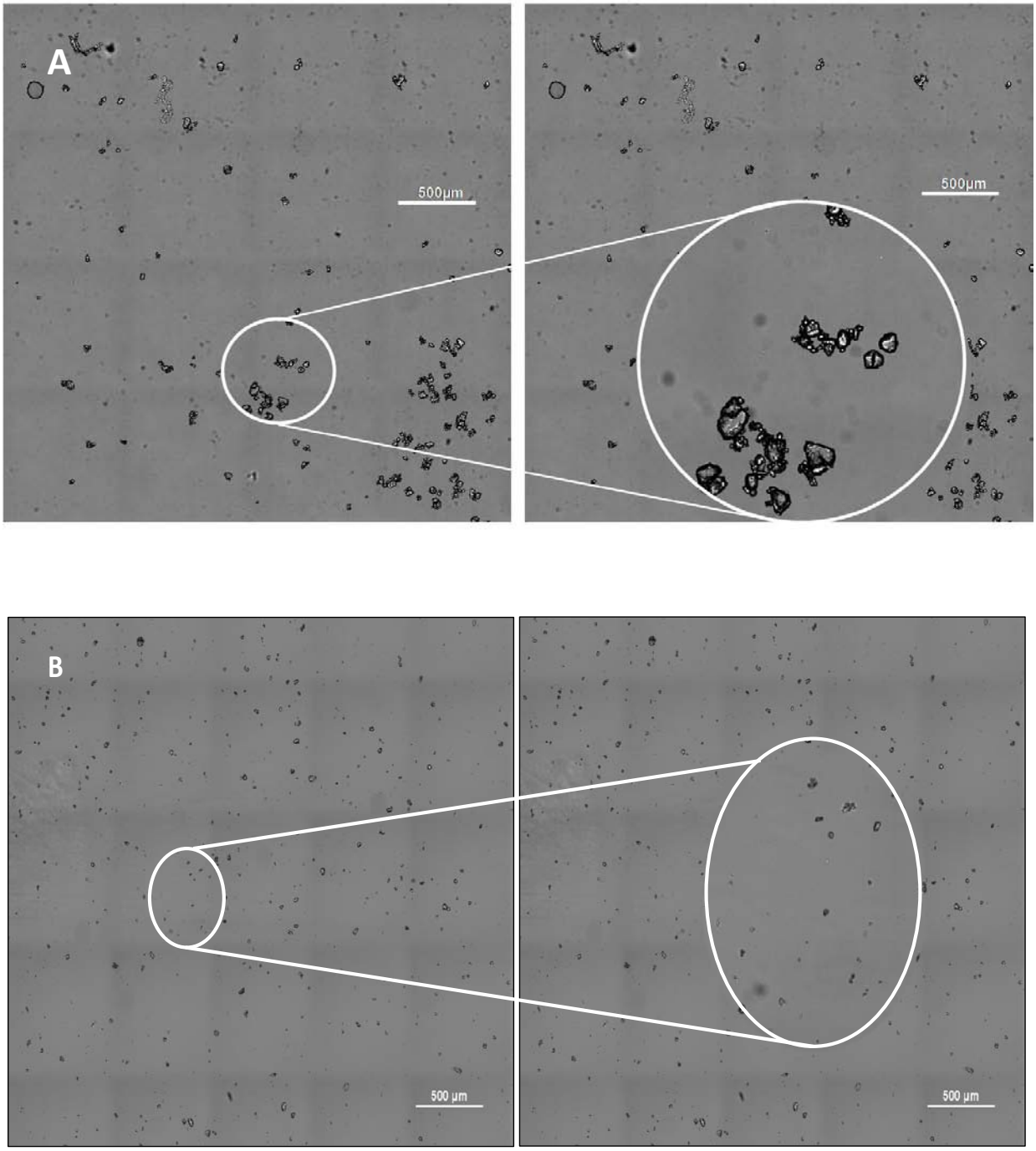


Figure 3– Particle size analysis images
A. Particle size analysis image of slide prepared without BSA, showing flocs of particulate DNT. B. Particle size analysis image of slide prepared with BSA, showing fa more homogeneous dispersion of particulate DNT.

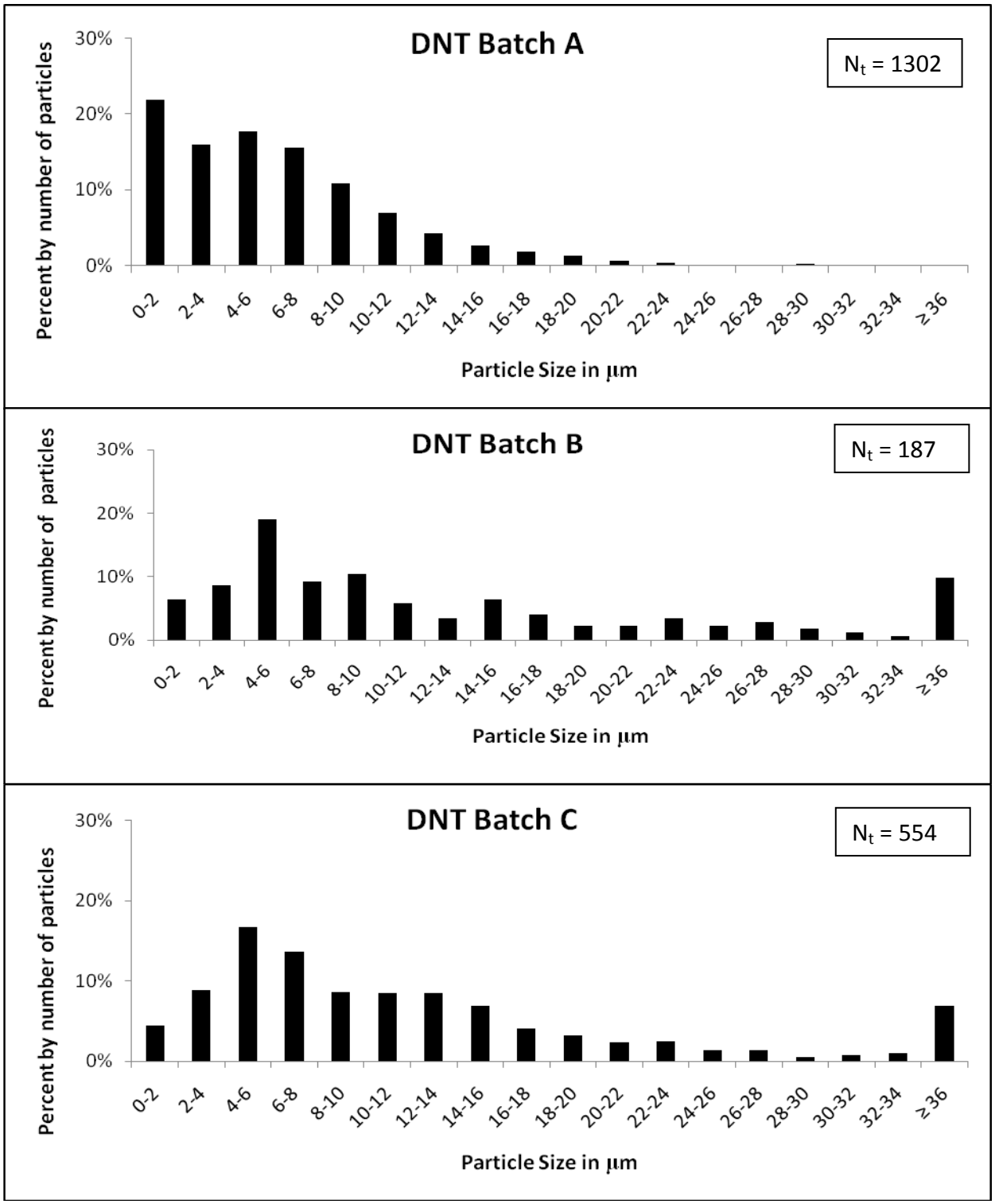


Figure 4– DNT particle size analysis
Results for particle size analysis of three different batches of DNT powder. N_t is the total number of particles counted per batch.

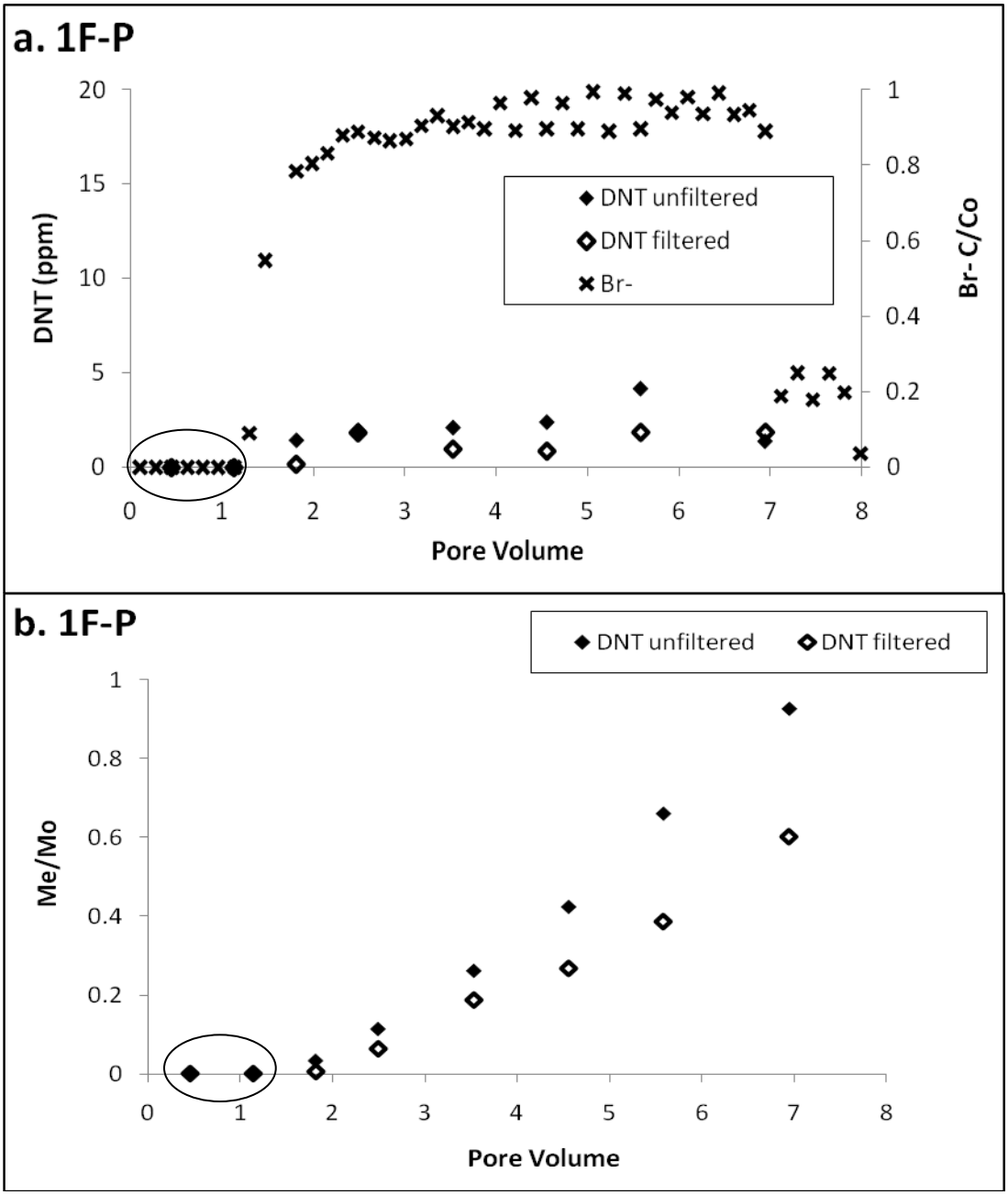


Figure 5 - Effluent results for suspended particulate DNT experiment 1F-P
In **5a**, presented as unfiltered and filtered sample DNT concentration and bromide concentration normalized to the influent concentration (C/C_o) versus pore volume of effluent. In **5b**, as cumulative DNT mass recovered in unfiltered and filtered samples normalized to total DNT input mass (M_e/M_o) versus pore volume of effluent. Samples were analyzed by method 8515. Analytical results were non-detect for circled data points.

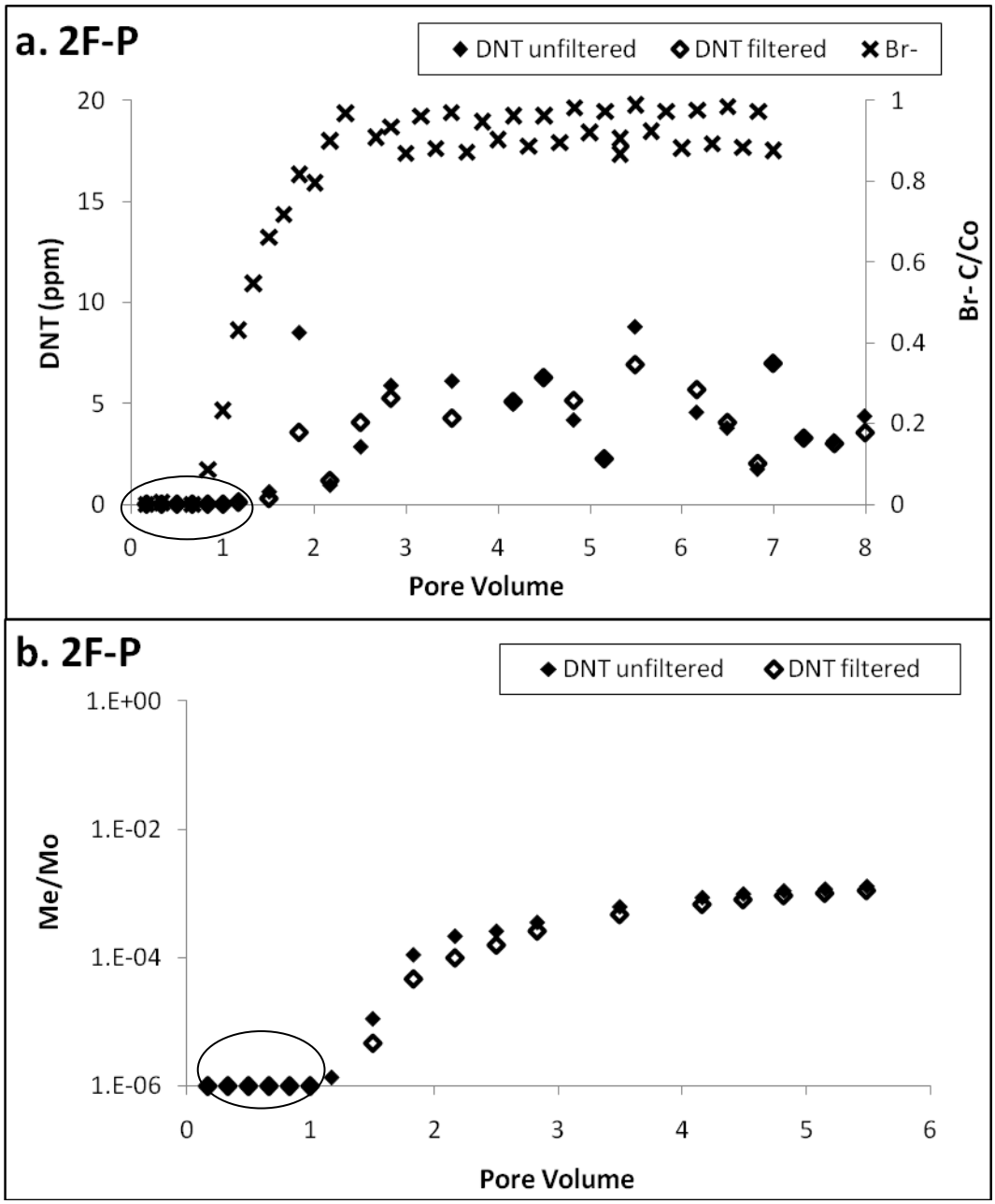


Figure 6 - Effluent results for particulate DNT surface application experiment 2F-P
In **6a**, presented as unfiltered and filtered sample DNT concentration and bromide concentration normalized to the influent concentration (C/C_o) versus pore volume of effluent. In **6b**, as cumulative DNT mass recovered in unfiltered and filtered samples normalized to total DNT mass applied to the column (M_e/M_o) versus pore volume of effluent. Samples were analyzed by method 8515. Analytical results were non-detect for circled data points.

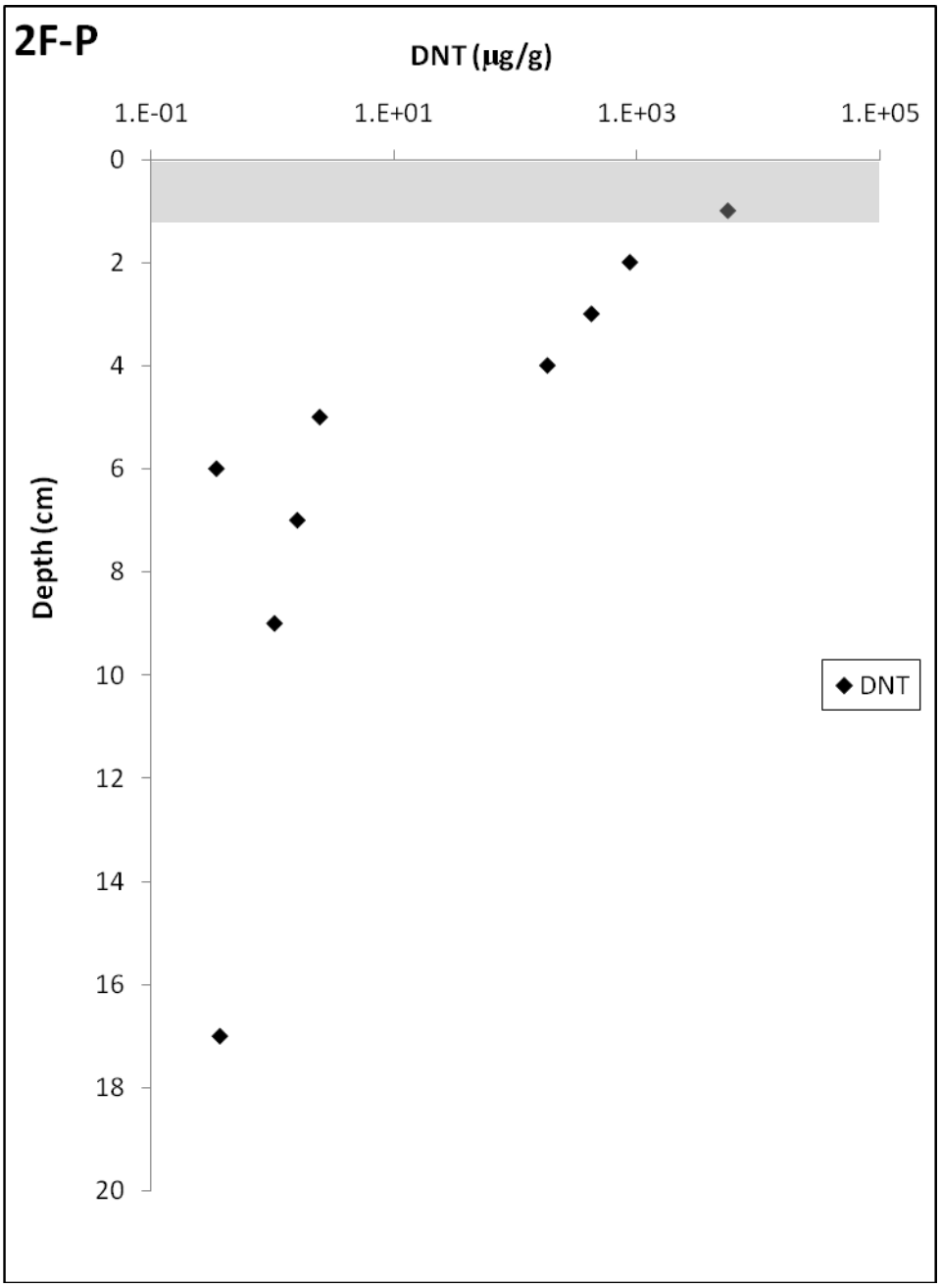


Figure 7 – DNT distribution in sand samples from particulate DNT surface application experiment 2F-P.
Presented as concentration (ug/g) versus depth (cm). Shaded area indicates depth of DNT surface application. Samples were analyzed by method 8515.

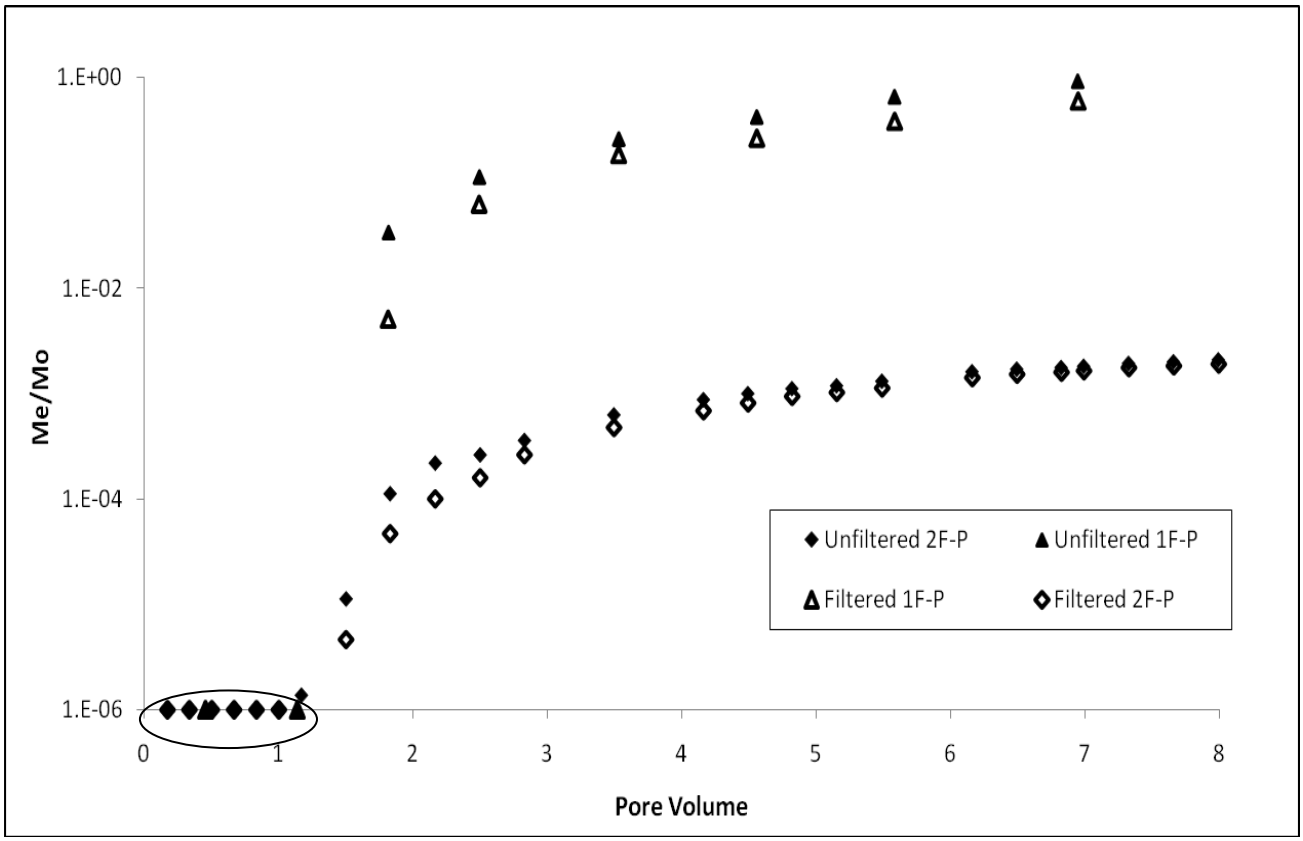


Figure 8 –Comparison of effluent results for suspended DNT experiment 1F-P and DNT particulate surface application experiment 2F-P

Presented as normalized cumulative mass recovered (M_e/M_o) from filtered and unfiltered samples versus pore volume of effluent. Samples were analyzed by method 8515. Analytical results were non-detect for circled data points.

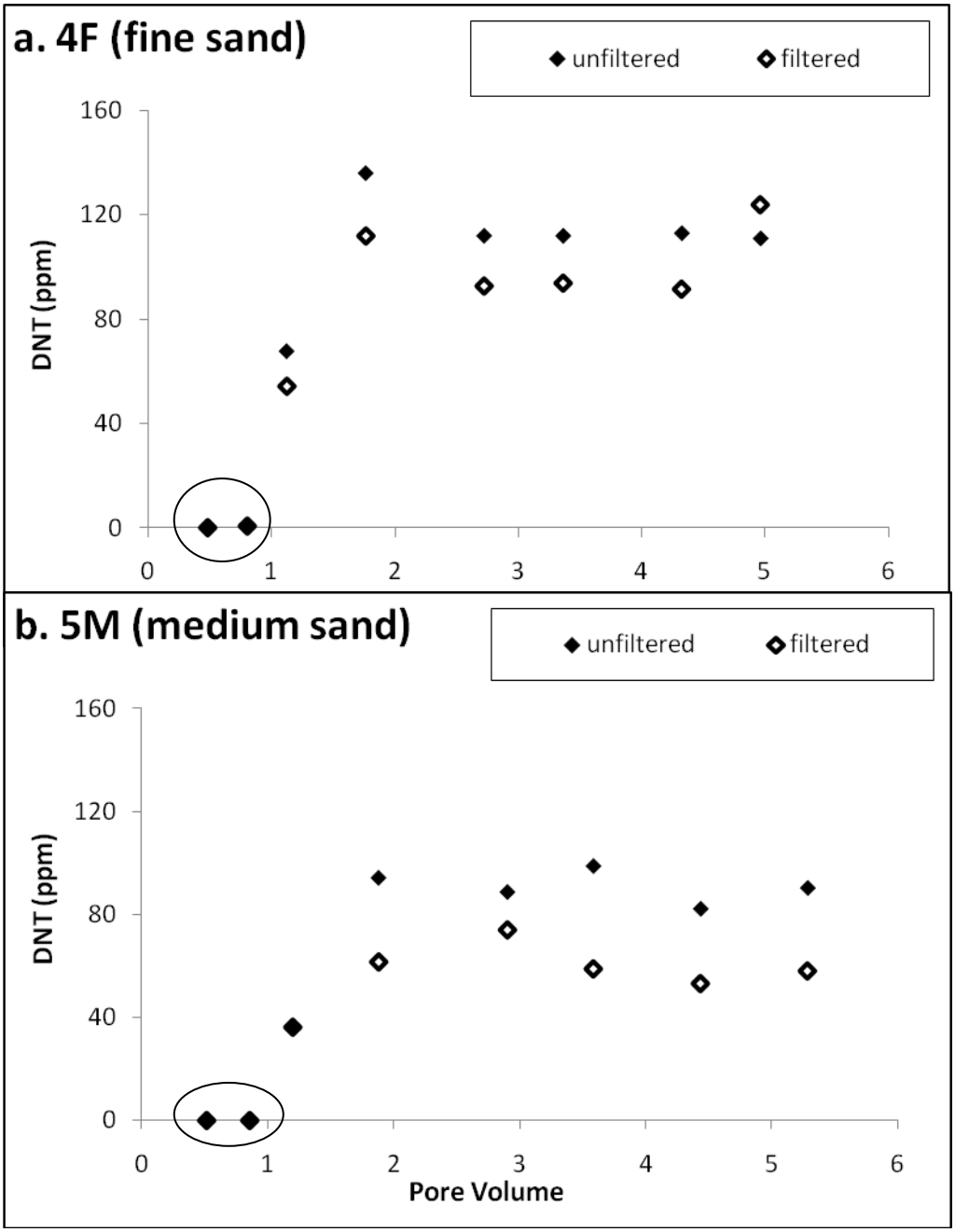


Figure 9- DNT concentrations for unfiltered and filtered effluent samples from DNT particulate surface application experiments in fine (3F-P) and medium (5M) sand.
In **9a**, presented as unfiltered and filtered sample DNT concentration versus pore volume of effluent. In **9b**, as cumulative DNT mass recovered in unfiltered and filtered samples normalized to total DNT mass applied to the column (M_e/M_o) versus pore volume of effluent. Samples were analyzed by method 8330. Analytical results were non-detect for circled data points.

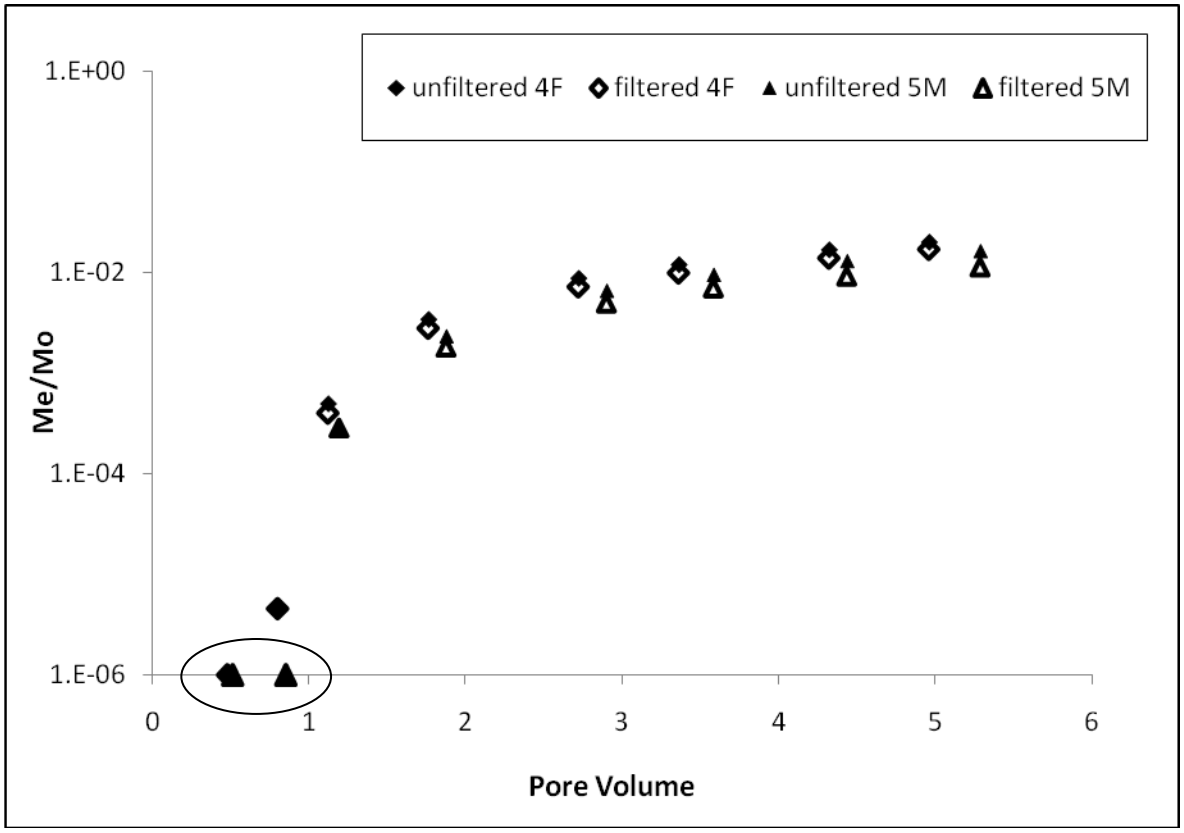


Figure 10 - Comparison of effluent results for particulate DNT surface application experiments in fine (4F) and coarse (5M) sand.
Presented as normalized cumulative mass recovered (M_e/M_o) from filtered and unfiltered samples versus pore volume of effluent. Samples were analyzed by method 8330. Analytical results were non-detect for circled data points.

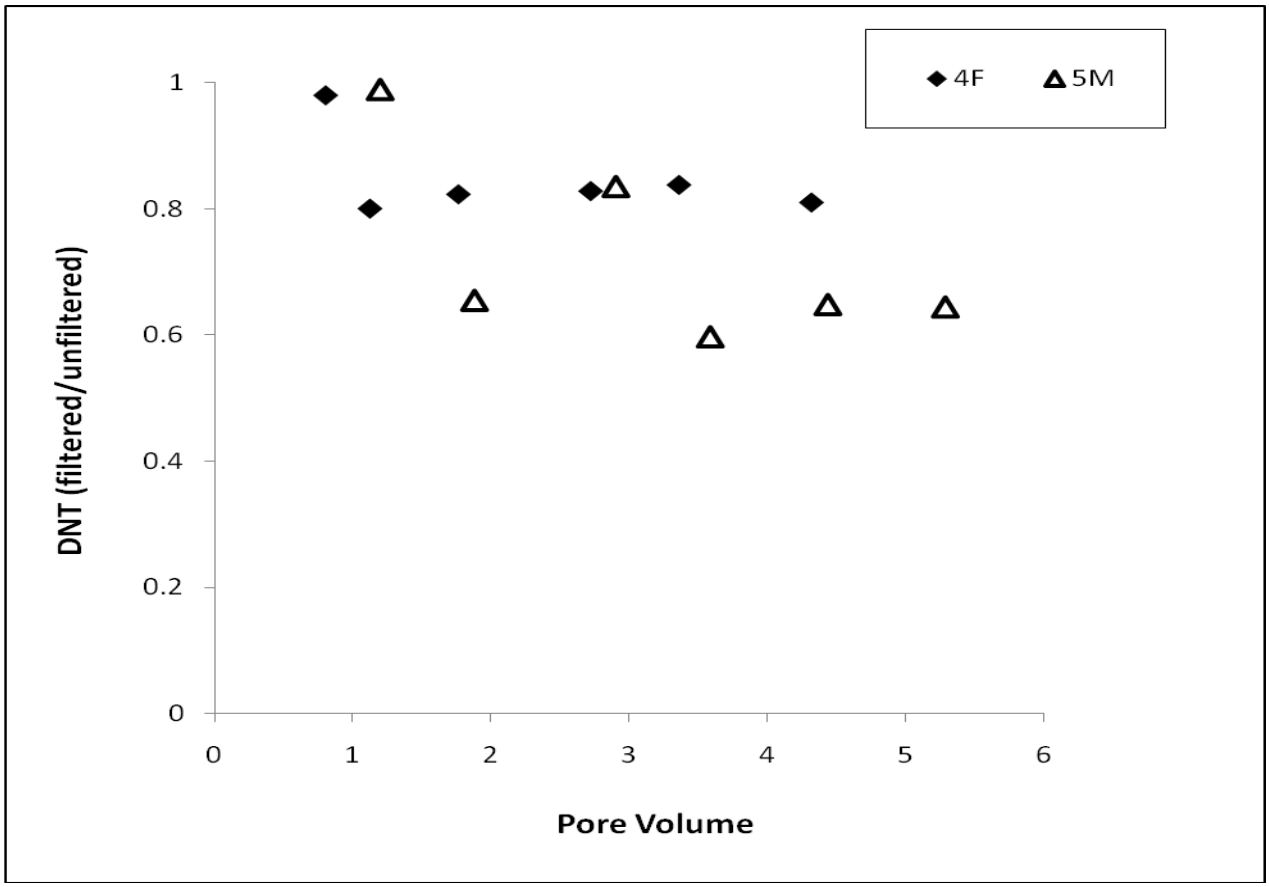


Figure 11- Ratio of filtered to unfiltered DNT concentrations in effluent samples from DNT particulate surface application experiments in fine (4F) and medium (5M) sand.
Presented as the ratio of filtered to unfiltered DNT concentration versus pore volume of effluent. Samples were analyzed by method 8330.

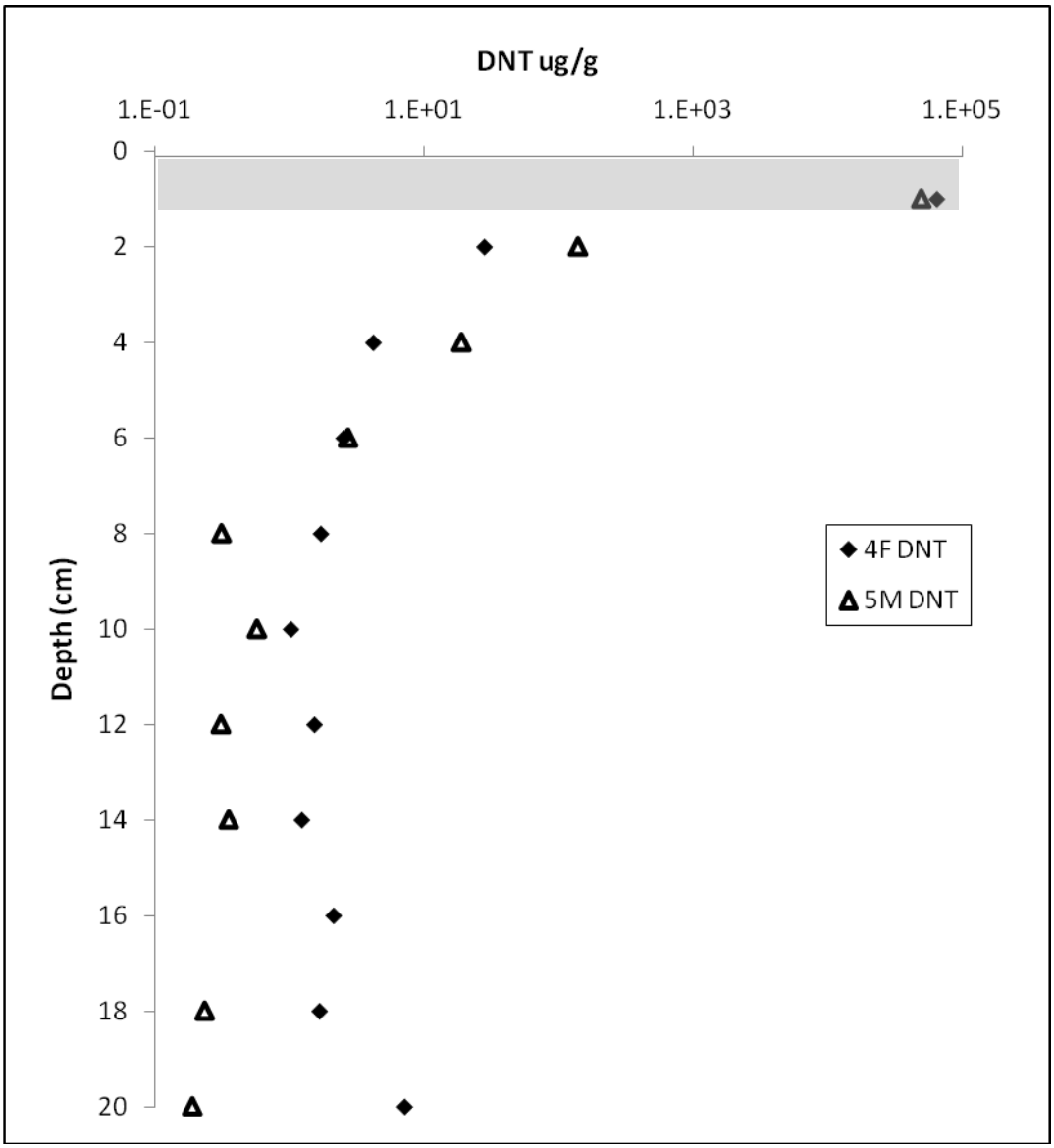


Figure 12 – Comparison of the DNT distribution in sand samples from particulate DNT surface application experiments in fine (4F) and coarse (5M) sand
Presented as DNT mass recovered per gram of sand in each 1 cm segment of sand (μg/g) versus depth. Shaded area indicates depth of DNT surface application. Samples were analyzed by method 8330.

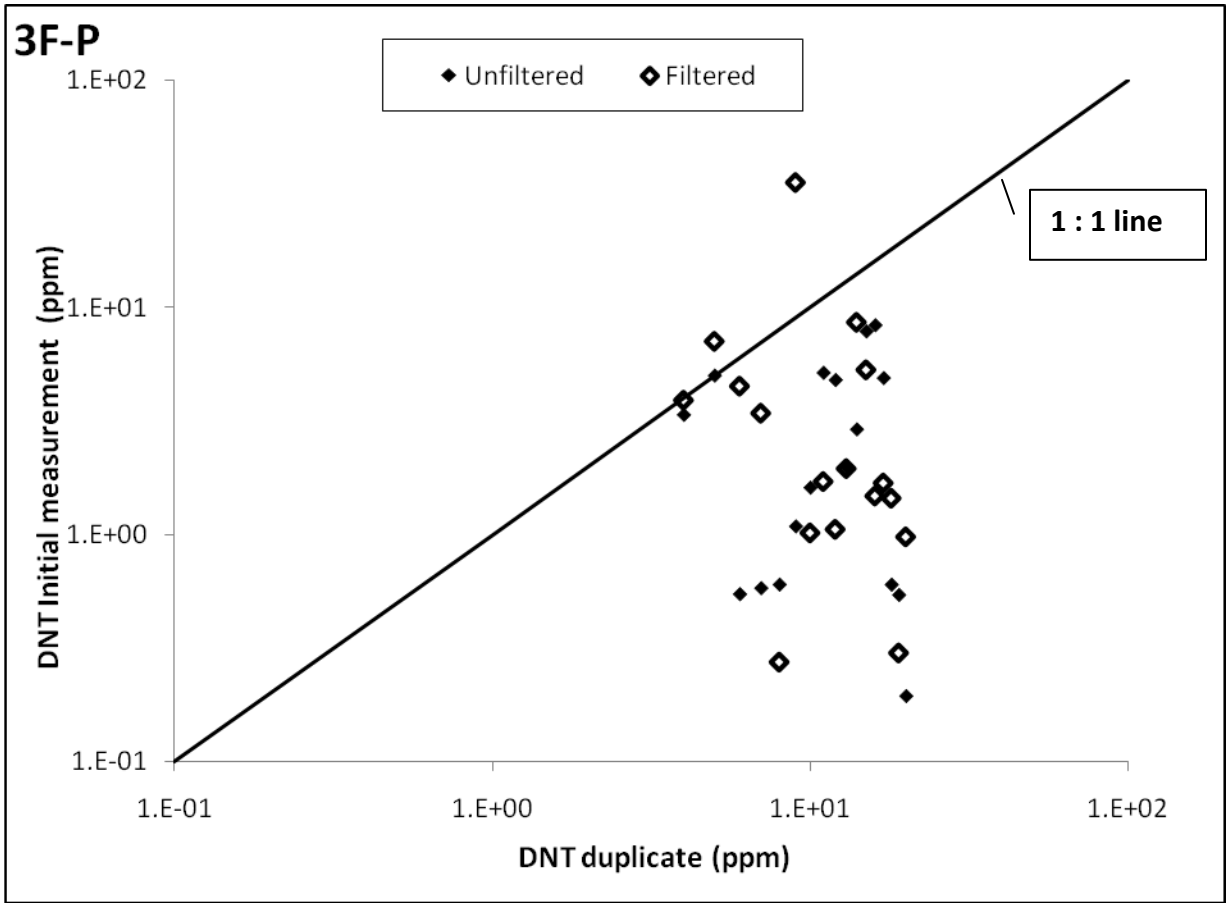


Figure 13 – Testing the reproducibility of analytical method 8515.
Analytical results from 8515 analysis of filtered and unfiltered samples and duplicates from DNT particulate experiment 3F-P, presented as DNT concentration (ppm) in unfiltered and filtered samples versus DNT concentrations (ppm) in their respective duplicate samples.

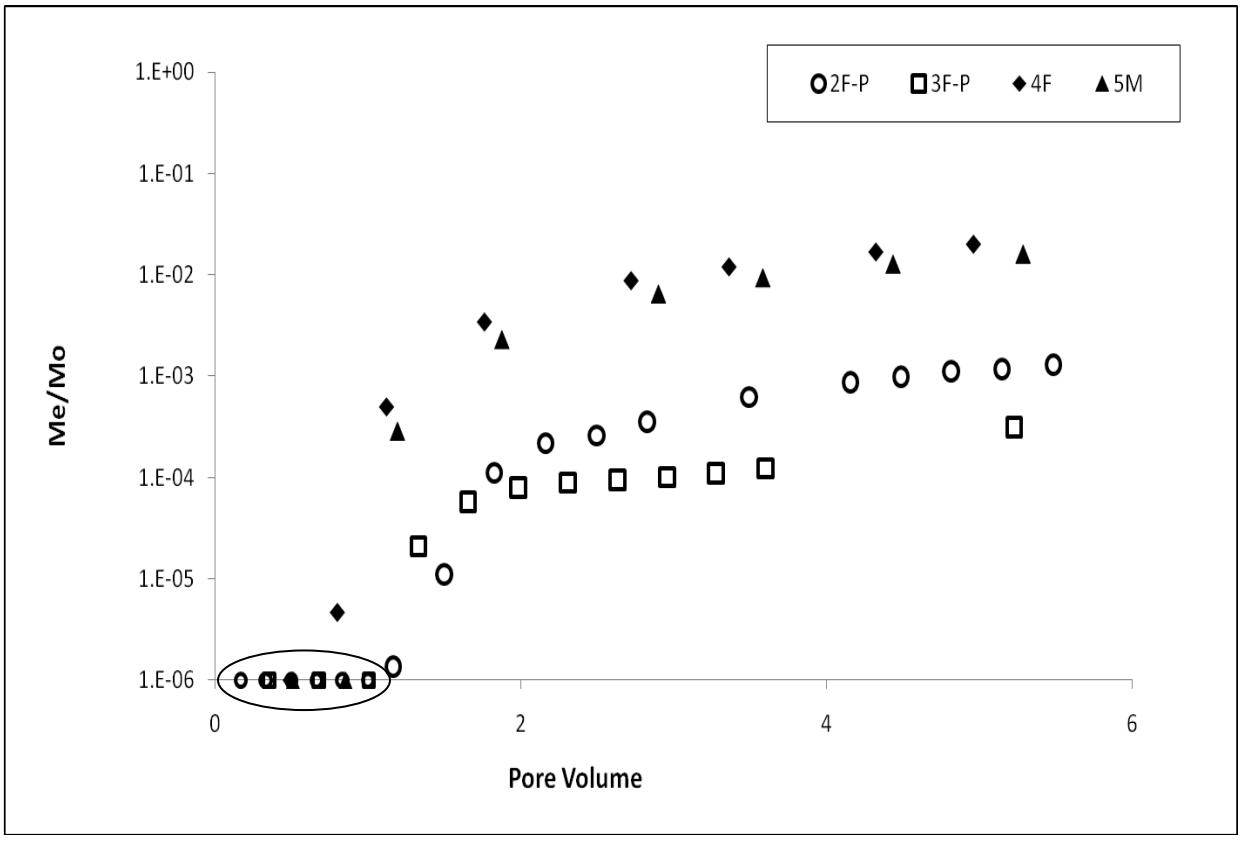


Figure 14 – Comparison of effluent results for all four particulate DNT surface application experiments

Presented as normalized cumulative mass recovered (Me/Mo) from filtered and unfiltered samples versus pore volume of effluent. Samples from 4F and 5M were analyzed with method 8330. Samples from 2F-P and 3F-P were analyzed with method 8515. Analytical results were non-detect for circled data points.

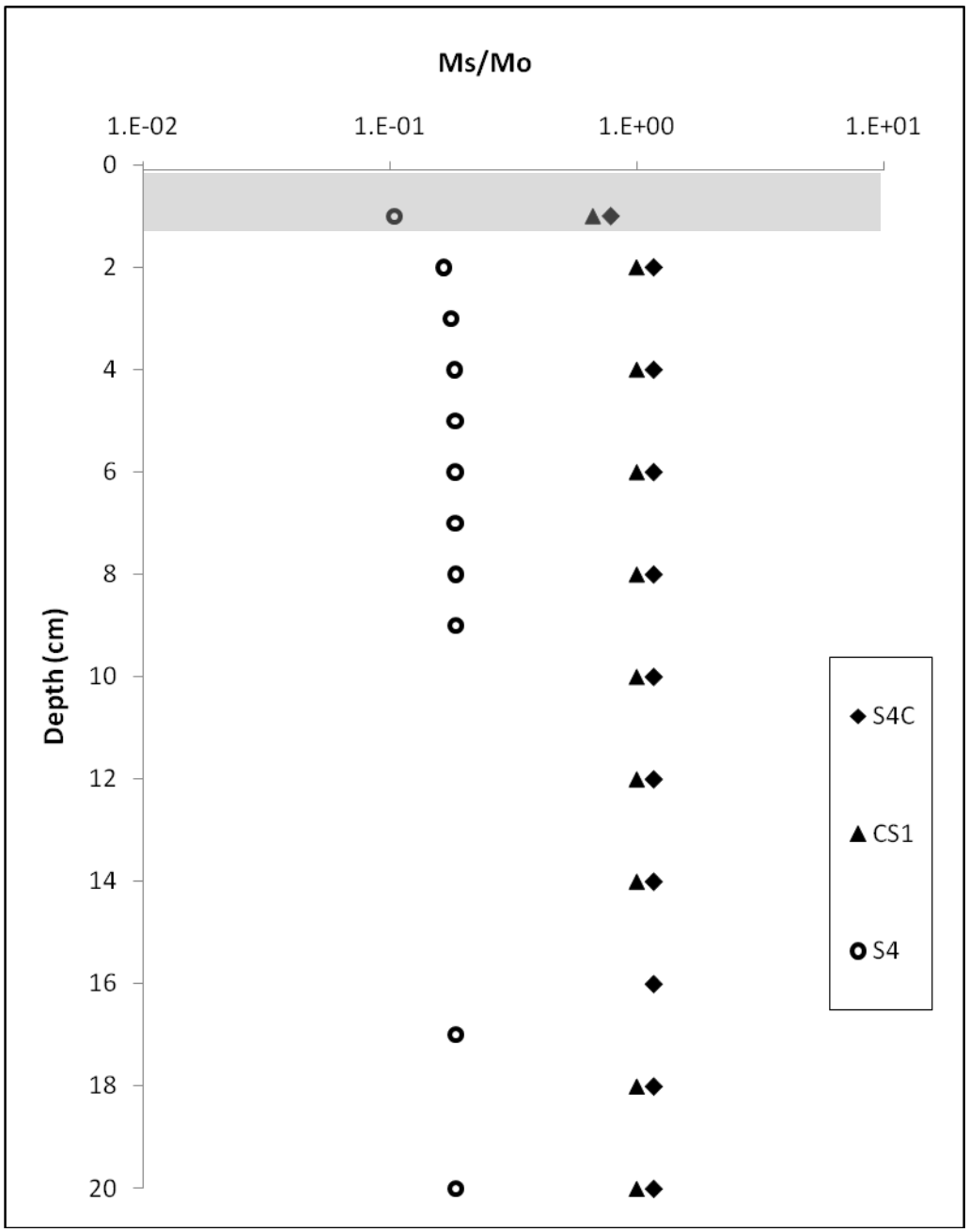


Figure 15 – Comparison of the DNT distribution in sand samples from particulate DNT surface application experiments 2F-P, 4F, and 5M
Presented as cumulative DNT mass recovered in each 1 cm segment of sand normalized to the initial DNT mass applied to the column (Ms/Mo) versus depth. Shaded area indicates depth of DNT surface application. Samples from 4F and 5M were analyzed with method 8330. Samples from 2F-P were analyzed with method 8515.

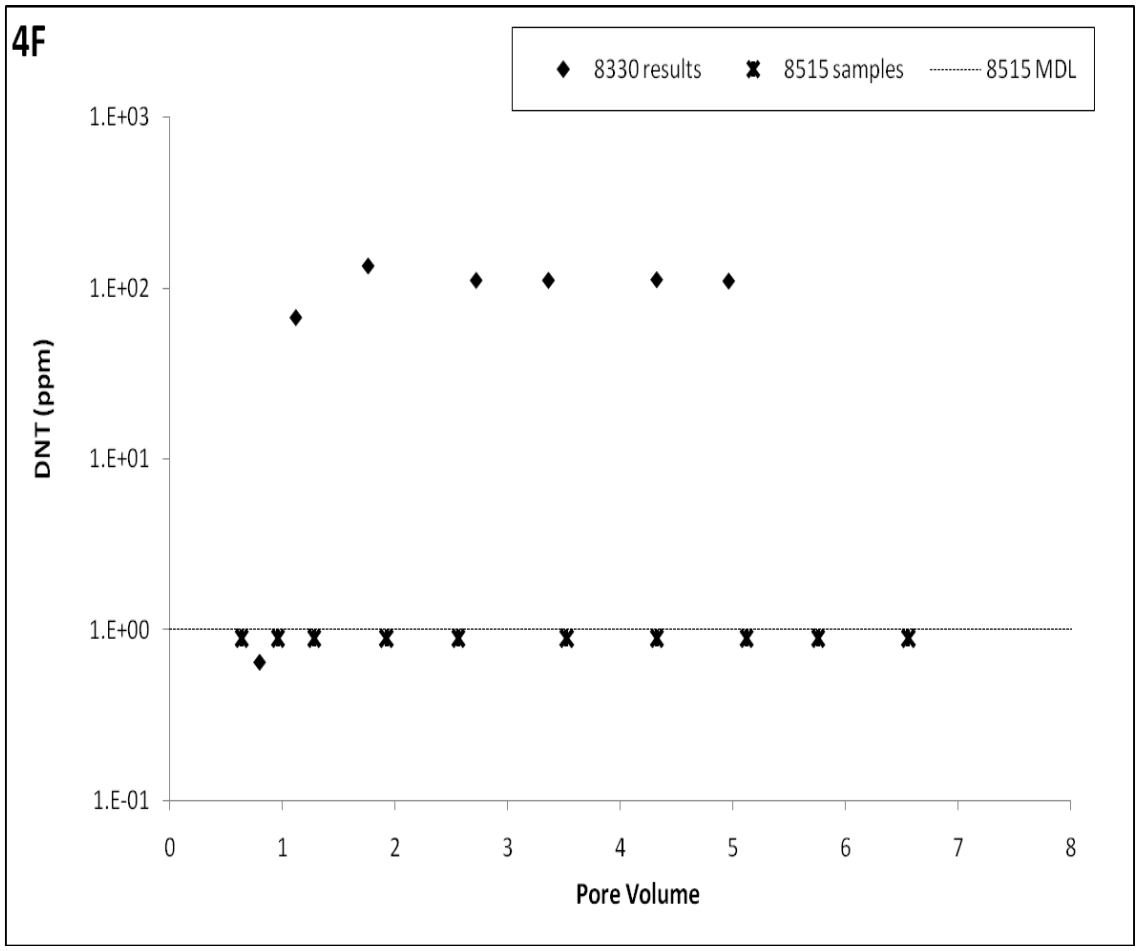


Figure 16 –Comparison of results for 4F effluent samples analyzed by methods 8515 and 8330. Presented as concentration (ppm) versus pore volume of effluent. All samples analyzed with method 8515 were below the minimum detection limit (MDL) of 1 ppm. In contrast, analyses by method 8330 of effluent from alternate pore volumes indicate detectable DNT concentrations.

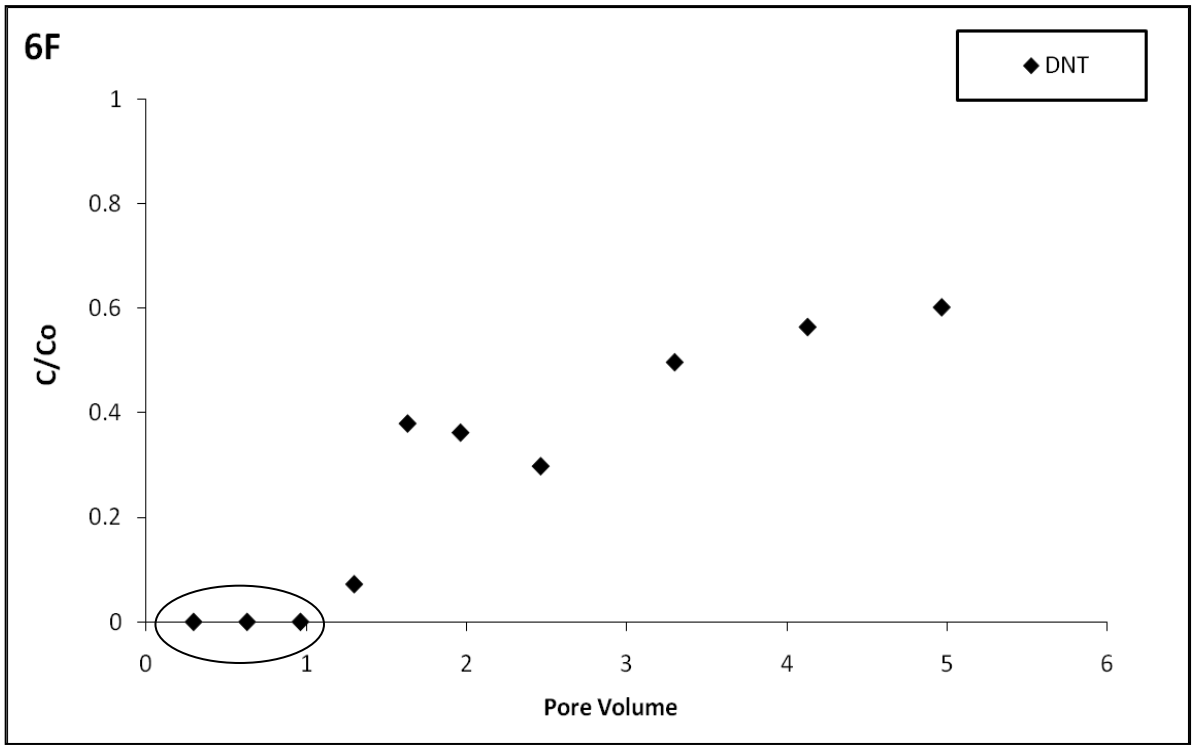


Figure 17 - DNT concentrations for filtered effluent samples from dissolved phase experiment 6F
Presented as concentration normalized to the influent concentration (C/C_o) versus pore volume of effluent. Samples were analyzed by method 8330. Analytical results were non-detect for circled data points.

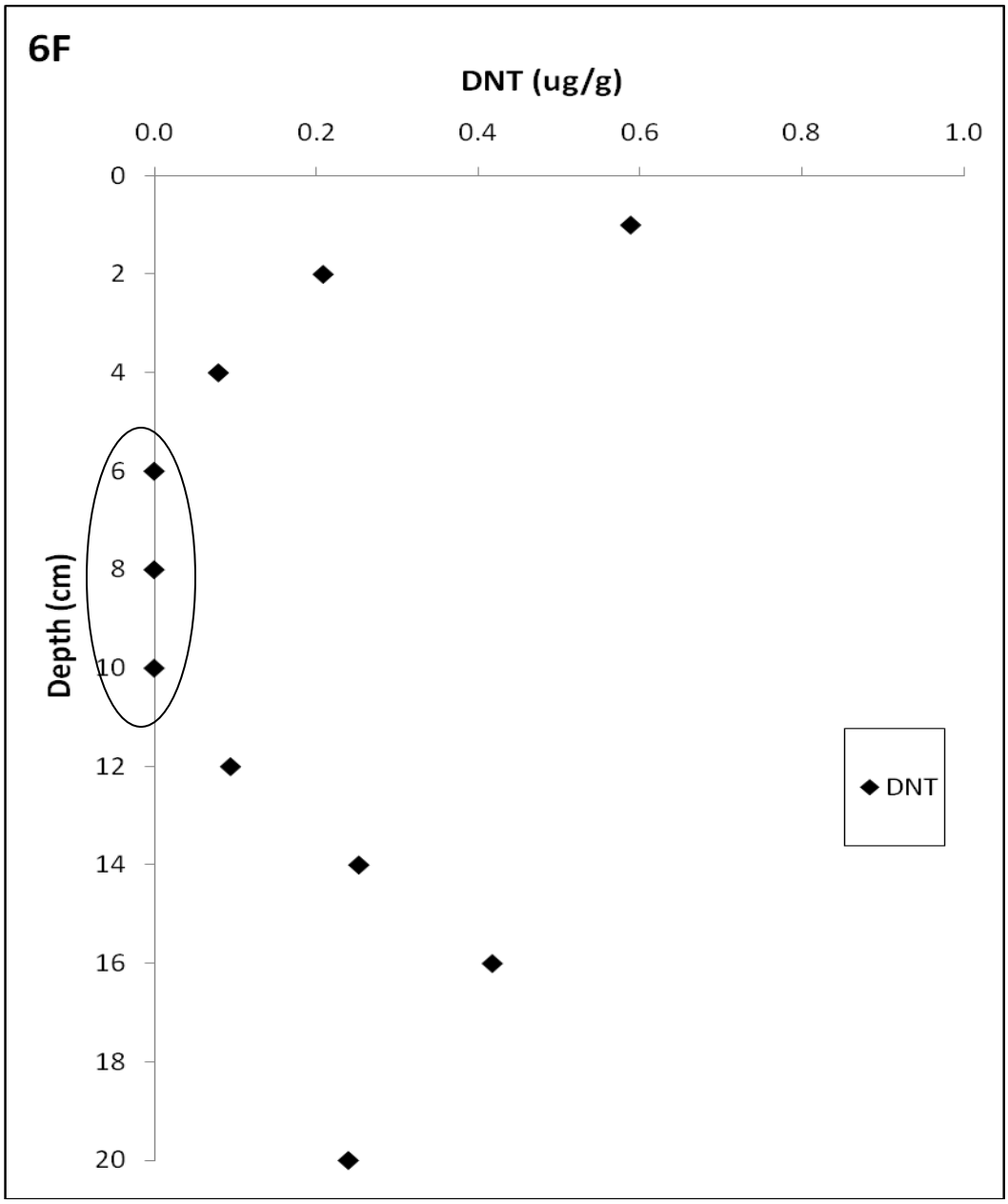


Figure 18 - DNT distribution in sand samples from dissolved phase experiment 6F
Presented as concentration (ug/g) versus depth (cm). Samples were analyzed by method 8330. Analytical results were non-detect for circled data points.

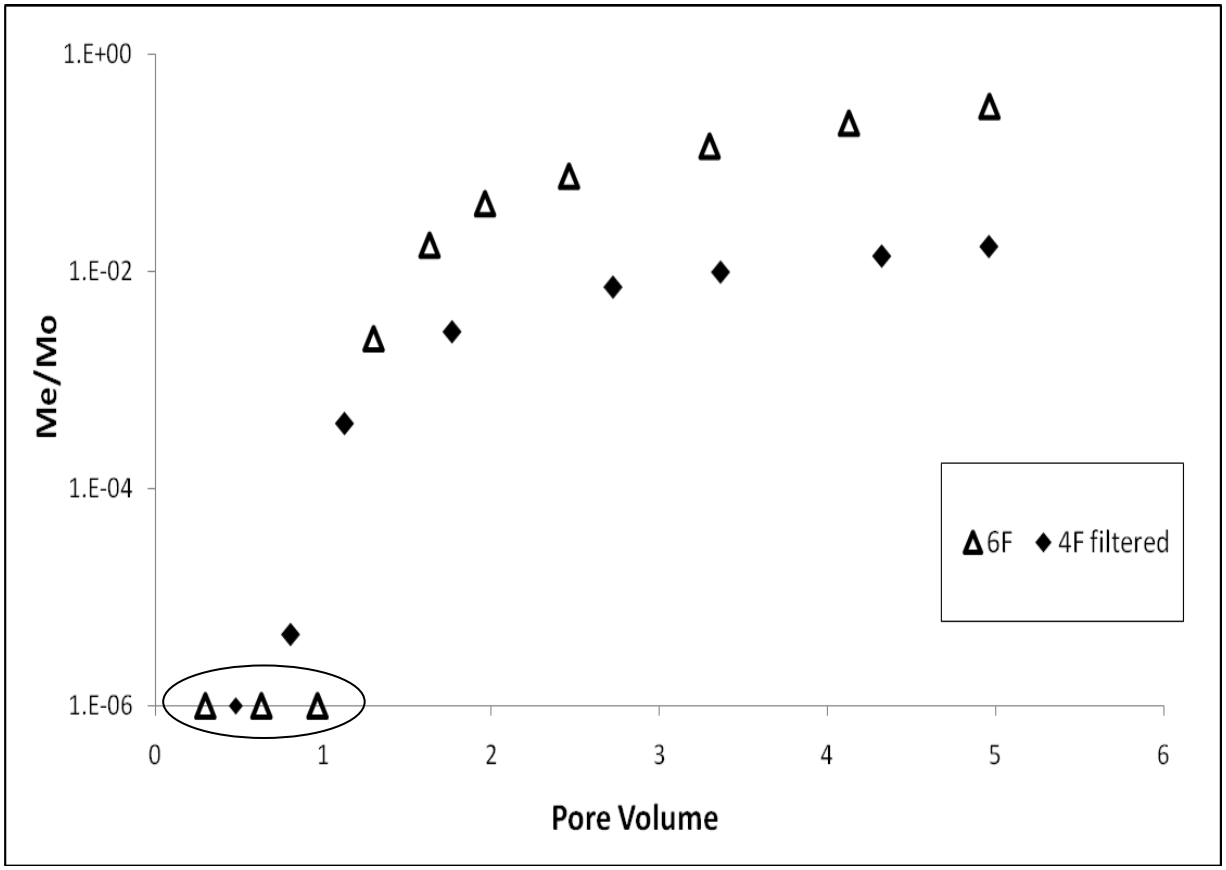


Figure 19 – Comparison of effluent results for dissolved phase DNT experiment 6F and particulate DNT surface application experiment 4F, both in fine sand.
Presented as normalized cumulative mass recovered (Me/Mo) from samples (filtered for 4F) versus pore volume of effluent. Samples analyzed with method 8330. Analytical results were non-detect for circled data points.

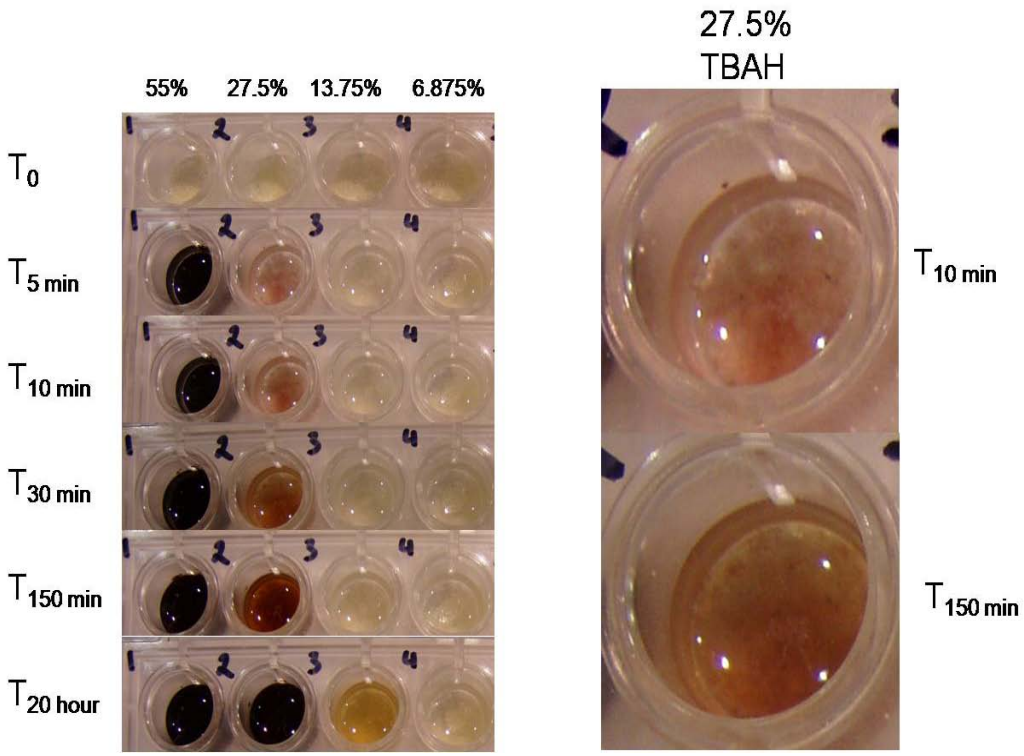


Figure 20 - Time series of images of DNT powder reacting with different TBAH concentrations
The left hand image depicts DNT colorimetric reactions to different concentration levels of the TBAH chemical stain imaged over a period of 20 hours. The TBAH concentrations are listed above the image and correspond to the column of samples below. The duration of reaction time is listed on the lefthand side of the image and correspond to the samples in the rows to the right. The right hand figure is a close up image of the 27.5% TBAH concentration reaction after 10 min and 150 min.

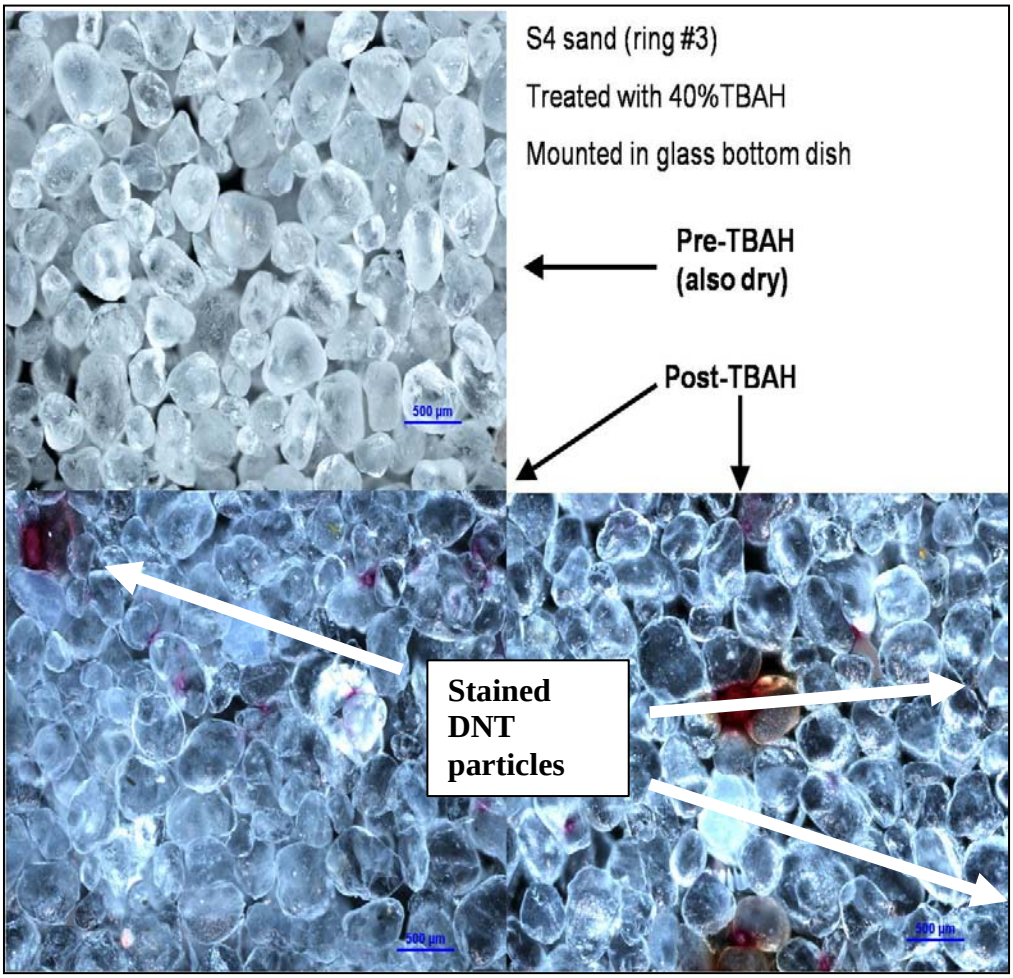


Figure 21 - Image of a sand sample from column experiment 2F-P
Before (top image) and after (two bottom images) the application of the TBAH chemical stain. The darker grains (indicated by the white arrows) are stained DNT particles.

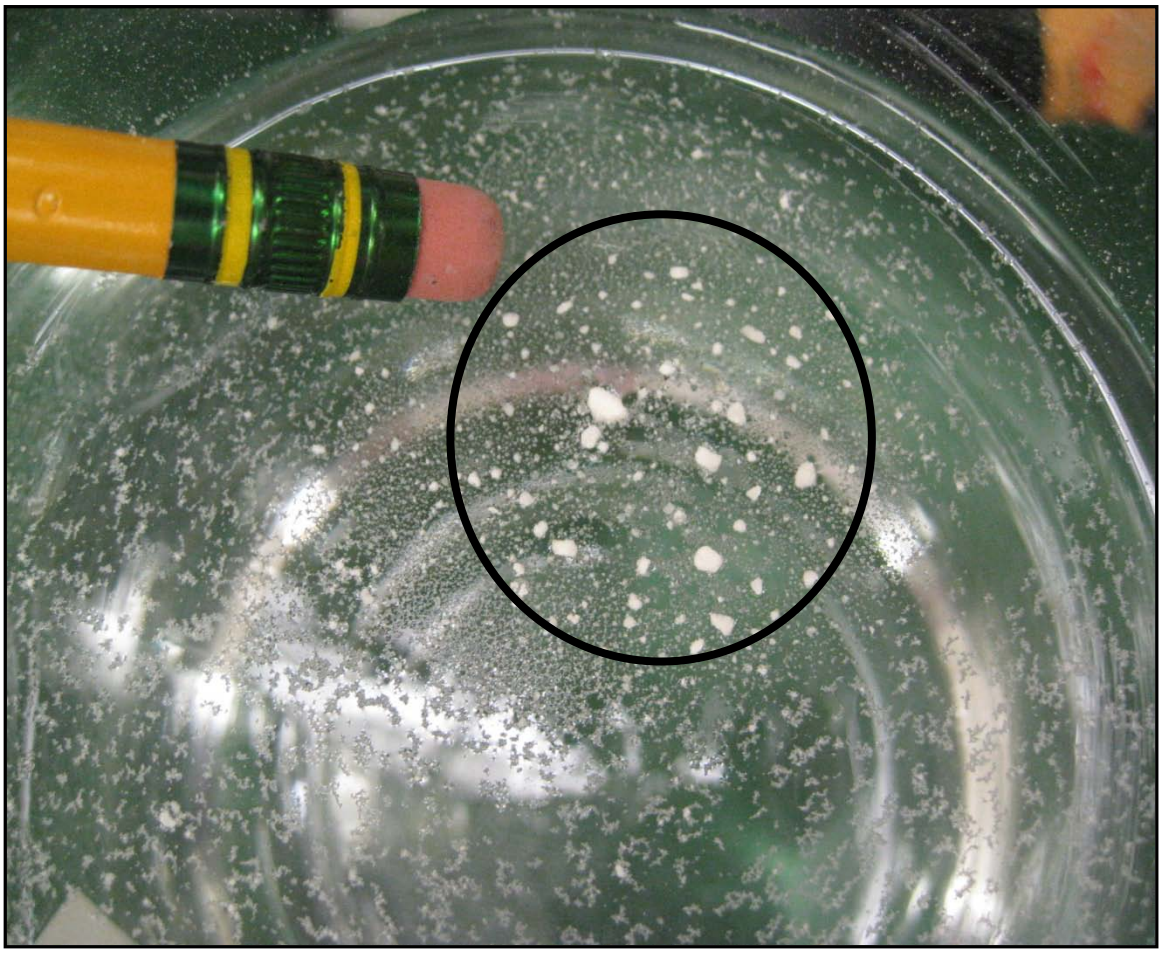


Figure 22 – Image of DNT particle aggregates in the influent solution with 1% BSA

Tables

Table 1: Chemical properties of Composition B constituents and ER surrogate

Compound	Distribution coefficient[1] (cm^3/g)	Solubility[2] (mg/L)
2,6-DNT	0.7 to 3.56	204
TNT	0.29 to 2.4	117
RDX	0.05 to 0.65	46.6
HMX	0.2 to 0.35	3.95

1. Distribution coefficient values are from Dontsova et al. (2006) and Clausen et al. (2006) for TNT, RDX and HMX and from 0.07 to 3.56 L/kg from Pennington et al. (2003) for 2,6-DNT.

2. Solubility values are from Morley et al. (2006) for TNT, RDX and HMX (at 22^{o}C) and from Luning Prak and O'Sullivan (2007) for 2,6-DNT (at 24 ^{o}C).

Table 2: Summary of column transport experimental conditions

Experiment ID	Tracer Application Technique	Tracer	Sand Type	Porosity	K_{sat} cm/s
M1	Suspension	Microspheres & Br	Fine	0.31	3.34E-03
M2	Mixed w/sand	Microspheres & Br	Fine	0.32	4.06E-02
M3	Mixed w/sand	Microspheres & Br	Fine	0.32	1.35E-01
1F-P	Suspension	[1]DNT & Br	Fine	0.30	4.99-02
2F-P	Mixed w/sand	[1]DNT & Br	Fine	0.32	4.12E-02
3F-P	Mixed w/sand	[1]DNT	Fine	0.33	1.16E-01
4F	Mixed w/sand	[2]DNT	Fine	0.33	1.18E-01
5M	Mixed w/sand	[2]DNT	Medium	0.31	3.55E-01
M4	Mixed w/sand	Microspheres & Br	Medium	0.32	3.54E-01
6F	Dissolved	[2]DNT	Fine	0.32	1.45E-01

1 DNT analysis performed with EPA Method 8515 (colorimetric)

2 DNT analysis performed with EPA Method 8330 (HPLC)

Table 3: Mass balance results for DNT tracer experiments

	Preliminary Experiments using Method 8515			Experiments using Method 8330		
	1F-P	**2F-P**	**3F-P**	**4F**	**5F**	**6F**
Total Mass Applied to Column[1] (mg)	0.28	300	673	468	431	1.3
Mass Recovered in Effluent (mg)						
- Total	0.259 (92.7%)	0.528 (0.18 %)	1.43 (0.24 %)	9.25 (2 %)	6.98 (1.6 %)	0.571 (43.9%)
- Dissolved	NA[2]	NA[2]	NA[2]	7.89 (1.69 %)	4.85 (1.13%)	NA
- Particulate	NA[2]	NA[2]	NA[2]	1.36 (0.29 %)	2.13 (0.49 %)	NA
Mass Recovered in Sand (mg)	0	55.3 (18.4%)	149.9 (22.3 %)	549.0 (117.3%)	428.9 (99.4 %)	0.02 (1.6%)
Total Mass Recovered in Effluent and Sand (mg)	0.259 (92.7%)	55.8 (18.6%)	151.33 (22.5 %)	559.2 (119 %)	435.9 (101 %)	0.59 (45.5%)

Table 2 presents the mass balance results for the DNT tracer experiments. Total effluent values were determined using the unfiltered effluent sample concentration data. Likewise, the dissolved values are from the filtered effluent sample concentration data and the particulate values are inferred from the difference between the total and dissolved values.

1- For each experiment, the total mass is the amount of DNT applied to the top of the columns with the exception of suspended DNT experiment 1F-P and dissolved phase DNT experiment 6F. Total mass for 1F-P and 6F is based on the DNT concentration in the influent reservoir (from unfiltered samples) and the volume of influent solution applied to the column.

2 - Statistical analysis results indicate there is no significant difference between the filtered and unfiltered samples for these experiments.

Appendix B

Overview of Microsphere Experiments

Four microsphere experiments (M1-M4) were conducted, using different application techniques and two grain sizes of sand, to characterize the transport of a non-reactive (non-dissolving) compound for a qualitative comparison to the transport of the DNT particulate tracer. Experimental conditions are provided in **Table 1** of the main text.

Microsphere Properties

Multi-colored, carboxylate-modified latex, fluorescent microspheres (0.2 µm 0.5µm, 1µm, and 2µm green; and 1µm crimson or blue, and 2µm nile red) were obtained from Invirtrogen. All microspheres are suspended in a 2 mM azide solution of distilled water with concentration of 2% solids. The microspheres are relatively non-reactive and are characterized as hydrophilic by the manufacturer. As non-sorbing, non-dissolving particles, microspheres provide a comparison to the transport behavior of the potentially reactive and soluble DNT. Preliminary particulate tracer experiments M1 and M2 were conducted with green microspheres, while spheres with different colors for each size were used for experiments M3 and M4. Each of these experiments was performed using 0.5, 1.0, and 2.0 µm size spheres, with the exception of M1, which also included the 0.2 µm size.

Microsphere Detection Methods

Flow Cytometry

Effluent samples from the microsphere experiments were analyzed for particulate content and size distribution using an Accuri 66 flow cytometer. Samples are homogenized with a vortex mixer and then the flow cytometer withdraws a 30 µL sub-sample for analysis. Flow cytometry is quantitative detection method based on six parameters: forward scatter; a measurement of particle size, side scatter; a measurement of granularity (e.g. inter-particle vesicles), and four channels of fluorescence.

Due to electronic noise associated with the photomultiplier tube (PMT) detectors, the practical minimal particle size for the flow cytometer used in this study is 1 μm. The default threshold for forward scatter detection is 80,000. In order to detect the submicron microspheres (0.2 to 0.5 μm), the forward scatter threshold was reduced to 10. At this lowered threshold there is a significant amount of noise (1000's of events/ul). While the larger microspheres can still be detected and quantified on a plot of forward scatter versus side scatter, the submicron particles, though detectable, are impossible to differentiate from the noise based on size and granularity alone. However, the smaller spheres can be identified as the highly fluorescent particles within the "noise region" of the forward vs. side scatter profile.

Fluorescence microscopy

Sand samples from the microsphere experiments were mounted on slides and analyzed with widefield epifluorescence microscopy. 3D image stacks were captured, deconvolved, and analyzed with image analysis software. Quantitative analysis of microsphere concentration is based fluorescence intensity. Microsphere concentrations (Ns) are derived from three measurements: the average particle fluorescence volume (Vp), the size distribution fraction (Fs), and the total fluorescence volume for the sand sample (Vt), where:

$$Ns = \frac{Vt}{Vp} * Fs$$

Fluorescence volume is based on the volume of pixels in a given image data that meet a defined fluorescence intensity threshold. The average particle fluorescence volume (Vp) for each size microsphere was measured in control experiments with custom software using a seeded-segmentation algorithm. Total fluorescence volume (Vt) and particle size distribution (Fs) were determined for each sand sample from the columns. Total fluorescence volume for the sand sample was measured using NIS-Elements software v3.0 (Nikon). To determine the size distribution (Fs) of microspheres in experimental samples, the image analysis software randomly selects fluorescent objects in the three dimensional image data. A user then rejects (as

unidentifiable), accepts (as an identifiable single sphere), or numerates (identifies it as 2, 3, or 4, etc objects touching/overlapping each other) the object.

Microsphere Tracer Experiments - Results

Microsphere Suspension Experiment – M1

Results for suspension experiment M1, with microspheres suspended in the influent reservoir, are presented in **Figure A1**. Values are plotted as the number of a given size microsphere counted per milliliter of effluent sample (#/ml), normalized to the concentration (#/ml) in the influent reservoir (Ne/No). Microsphere results are reported in terms of log reduction or removal, defined as the log value of the average plateau Ne/No. In addition to the 0.5, 1.0 and 2.0 μm size microspheres, 0.2 μm microspheres were also used in M1. However, flow cytometry and microscopy based detection techniques could not differentiate between the 0.2 μm and 0.5 μm size spheres. Because of this, the 0.2 μm size spheres were excluded from later experiments. For experiment M1 results, concentration values for the 0.5 and 0.2 μm spheres are combined. Flow cytometry results also indicated the detection of microspheres, at counts of approximately 100/mL, in background samples suggesting either cross-contamination of the background solution or some kind of interference with the analysis. The low concentrations reported for the early pore volume data is likely the result of the same interference.

The results for all microspheres sizes indicate similar degrees of attenuation. Log reductions for each size microsphere, calculated using plateau breakthrough concentrations versus the influent concentration in the reservoir, are summarized in **Table A1**. Both the 0.5/0.2 μm and the 2.0 μm spheres exhibit 2 log removal while the 1.0 μm spheres show slightly less attenuation with 1 log removal relative to the influent concentration. Paired t-test analysis of the 0.5/0.2 μm and the 2.0 μm spheres effluent data indicates at the 95% confidence interval that there is no significant difference between these populations.

The distribution of the microspheres in the sand column after the experiment is presented in **Figure A2**. Values are presented as the total number of a given size microsphere counted per

segment of sand normalized to the influent concentration (N_s/N_o). Each size microsphere exhibits a curvilinear decrease in concentration with depth. Throughout the column, the 2.0 μm spheres show the greatest degree of attenuation while the 1.0 μm spheres demonstrate the least. Mass balance calculations for M1 are presented in **Table A2**. The total percentage recovered for each size sphere is several magnitudes higher than expected. The poor mass balance for the microspheres in M1 sand samples raises questions about the reliability of the detection methods. Either the flow cytometry analysis underestimated the influent concentration or the fluorescence microscopy analysis overestimated the concentrations in the sand. The flow cytometry input concentration (~ 7E+06 total # of spheres/L) seems reasonable based on the volume of microsphere suspensions added to the influent solution. Microscopic image analysis was unable to differentiate between the 0.2 and 0.5 um diameter microspheres. This issue coupled with the use of a monochromatic (green) set of microspheres may be the source of error.

Microsphere surface application experiments – M2-M4

Three microsphere surface application experiments conducted in fine sand (M2 and M3) and medium sand (M4). Results for M2 are presented in **Figure A3** and results for experiments M3 and M4 are presented in **Figures A4a** and **A4b**, respectively. Values are plotted as concentration of a given size of microsphere normalized to the initial microsphere concentration (N_e/N_o) versus pore volume of effluent. N_e is the number of a given size microsphere per millimeter of effluent and N_o is the concentration of that size microsphere (#/ml of porewater) initially applied to the top centimeter of sand in the column. N_o was determined by fluorescence microscopy analysis of a subsample of the sand/microsphere mixture applied to the top of the columns. Experimental conditions were the same for each experiment with the exception that a higher concentration of BSA (2 g/L) was used unintentionally in M2.

Log reductions in concentration for each size microsphere, calculated using plateau breakthrough concentrations versus the influent concentration in the reservoir, are summarized in **Table A1**. In general, the results for effluent samples from M2 are comparable to those for M3, the other microsphere surface application experiment conducted in fine sand. There appears to be greater retention of the 0.5 μm microspheres in M3 versus M2. However, this variability could be due to

the increased concentration of the BSA or the poorly constrained input concentration. A comparison of results for fine sand experiment (M3) and the medium sand experiment (M4) shows a similar degree of removal for the 0.5 μm spheres. However, removal of the 1.0 and 2.0 μm spheres appears slightly increased in M4 relative to M3. Paired t-test statistical analyses of the M3 and M4 effluent data indicates, there was no significance difference between the 0.5 μm sphere reduction, and supports greater removal of the 1.0 and 2.0 μm spheres in M4 at the 95 % percentile level. (note: the M2 data were not subjected to statistical analyses because the effluent samples represent different pore volumes than those collected for experiments M4 and M3.)

Results for microsphere distribution in sand samples from M2 after the experiment are presented in **Figure A5**. Results for microsphere distribution in the M3 (fine sand) and M4 (medium sand) columns are presented in **Figure A6a and A6b**, respectively. Values are plotted as the concentration of a given microspheres (#/gram of sand) normalized to the pre-experimental concentration of microspheres in the top one centimeter of sand (N_s/ N_o) versus depth (cm). Results for M2 and M3 are similar, exhibiting a curvilinear decrease in microspheres with depth through the entire column. In both fine sand columns, the microsphere numbers decrease with depth through the entire column by a factor of 100 to 50 times. Concentrations in the medium sand (M4) also decreased with depth but only by a factor of less than 5 times. A comparison of the distribution of microspheres in M3 and M4 shows that 50% of the total number of microspheres applied is retained in the top 2 cm of the fine sand column, while in the medium sand column only 25% are retained proximal to the source area. Mass balance estimations for the microsphere surface application experiments are presented in **Table A2**. Similar to M1, the numbers of microspheres recovered in the M2 are much higher than 100%, suggesting possible inaccuracy in our microscopy detection method as previously mentioned. For M3 and M4, the results indicate high levels of attenuation in both medium and fine sands, with very low percentages of the spheres recovered in the effluent.

Normalized breakthrough curves for 1.0 μm microspheres from both the suspended microsphere experiment M1 and microsphere surface application experiments M3 and M4 are presented in **Figure A7**. The breakthrough curves for M3 and M4 plot erratically with no clear plateau. In both experiments there was an initial spike in microsphere counts followed by a dramatic drop.

After the initial spike, concentrations increase at a steady rate for approximately one pore volume before leveling out. In contrast, M1 appears to have a more typical breakthrough curve. It does not exhibit the initial concentration spike observed in the microsphere surface application experiments. In addition, attenuation of the microspheres is several magnitudes lower in M1 relative to M3 and M4. The distribution of 1.0 μm microspheres in sand samples from experiments M1 and M3 are plotted together in **Figure A8**, as normalized concentrations versus depth. Both curves exhibit similar trends but the retention of microspheres as several magnitudes higher in M1. However, as mentioned previously, overly high mass balance results for M1 suggest a problem with the analytical method resulting in an overestimation of the microspheres sand samples. This would create the appearance of a higher level of retention in the column.

Microsphere Experiments - Discussion

Breakthrough concentrations in effluent samples from microsphere suspension experiment M1 fall within the range of results presented in previous studies from microsphere transport experiments conducted under similar conditions. Knappett et al (2008), reported a normalized peak concentration of $< 10^{-4}$, representing complete attenuation, for 1.5 μm spheres in transport experiments conducted under similar conditions. Bradford and Bettahar (2006) observed normalized peak concentrations of 0.87 to 0.35 for 1 μm microspheres and 0.41 to 0.06 for 3.2 μm microspheres in the columns repacked with the same grain size sand. M1 removal rates for 0.5/0.2 um microspheres are also are comparable to the results of other studies (Lindqvist and Bengtsson, 1995). However, normalized breakthrough concentrations for all three surface application experiments are several magnitudes lower than those from experiment M1 and results reported for studies in which the microspheres were introduced in suspension. Results from these experiments also differed from previous studies that have reported enhanced microsphere transport in medium sands (Knappet et al, 2008).

In general, the spatial distribution of microspheres in the sand for both suspension and surface application experiments is similar to previously published results, exhibiting a curvilinear decrease in concentration with depth (Bradford and Bettahar, 2006). However, the decline in concentration is steeper for the surface application experiments. The lower effluent

concentrations and differences in spatial distribution in the sand columns from microsphere experiments M3 and M4 may be an effect of the surface application technique. The initial microsphere concentrations, as applied to the top centimeter of column, are relatively high compared to typical concentrations of microsphere suspensions applied in influent solutions. Although Bradford and Bettahar (2006) observed increased mass recovery in the effluent with increased input concentrations (that were similarly high) in the influent suspensions, it is possible that higher concentrations when applied directly to the top of a column might have the opposite effect. Microspheres suspended in an influent solution are relatively well dispersed and already in motion when they are introduced to the porous media. In contrast, microspheres applied directly to top of the columns are much more likely to be in contact with other spheres and/or sand grains. It seems probable that interactions resulting from such contact, combined with physical inertia imparted by the initial lack of flow, could inhibit the transport of the microspheres. This would explain both the lower breakthrough concentrations and the differences in spatial distribution of the spheres in the sand. Such factors might also diminish the impact of the increased grain size on particulate transport, especially since the number of microspheres applied in the medium experiment was slight higher than those applied to the fine sand columns.

Another interesting feature which might be an artifact of surface application, is the initial concentration spike observed in microspheres effluent data. This spike was not observed in experiment M1 and to our knowledge has not been reported by other column experiment studies. It is however, frequently observed in the field after storm events (Vesper & White, 2003; McCarthy & Shevenell, 1998).

Appendix B Figures

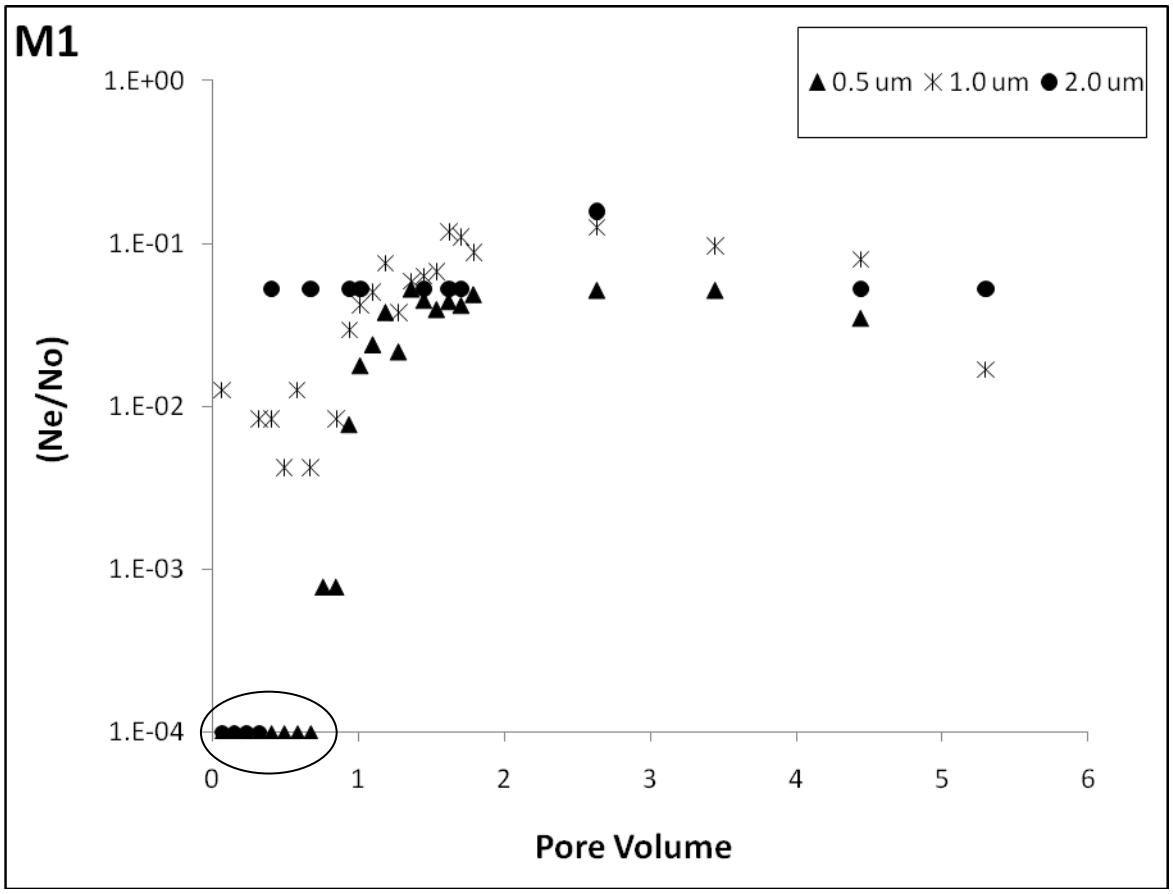


Figure A1: Effluent results for suspended microsphere experiment M1-
Presented as number of a given size microsphere counted per pore volume normalized to the concentration of that size microsphere in the influent solution (Ne/No). Analytical results were non-detect for circled data points.

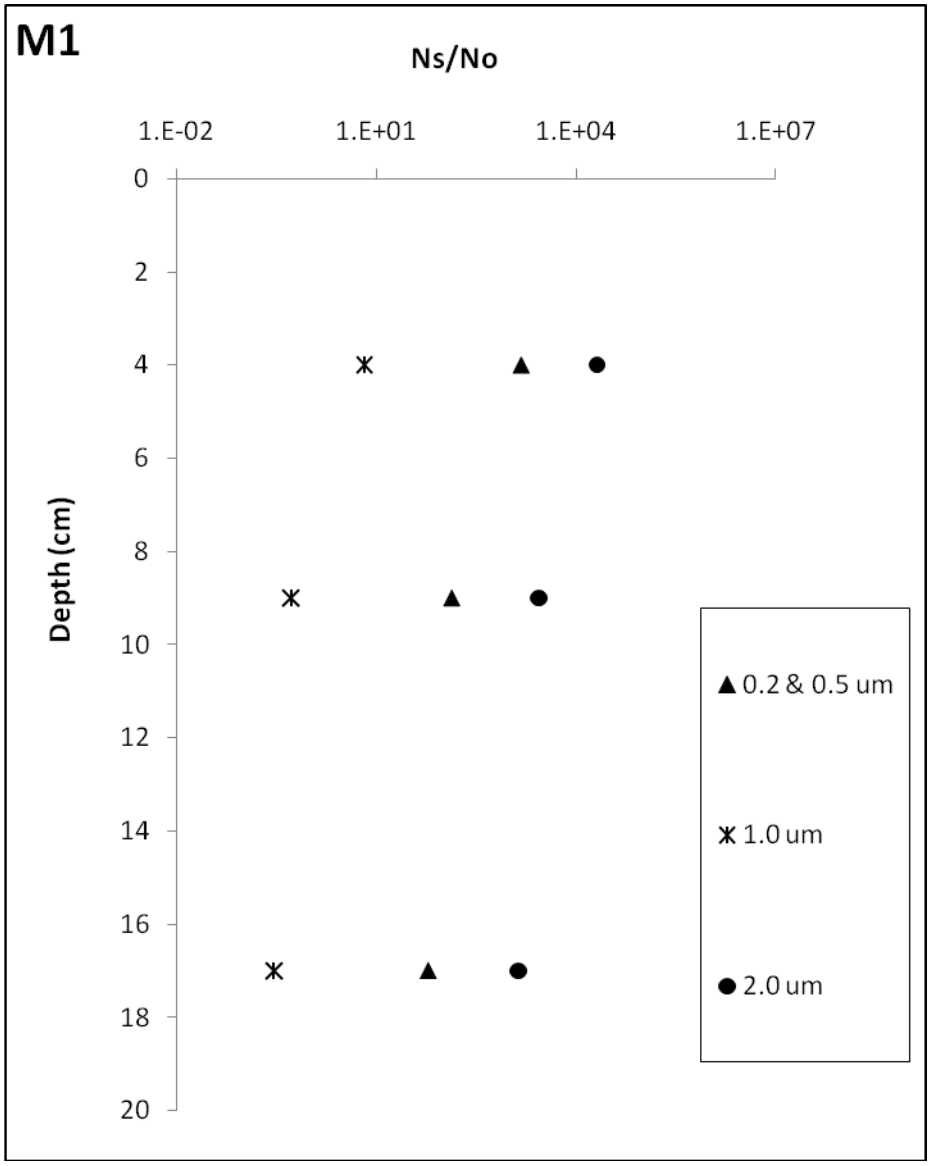


Figure A2: Distribution of microspheres in sand samples from suspended microsphere experiment M1

Values are presented as the total number of a given size microsphere counted per each centimeter segment of the column (~ 1 mL pore space) normalized to the influent microsphere concentration (Ns/No).

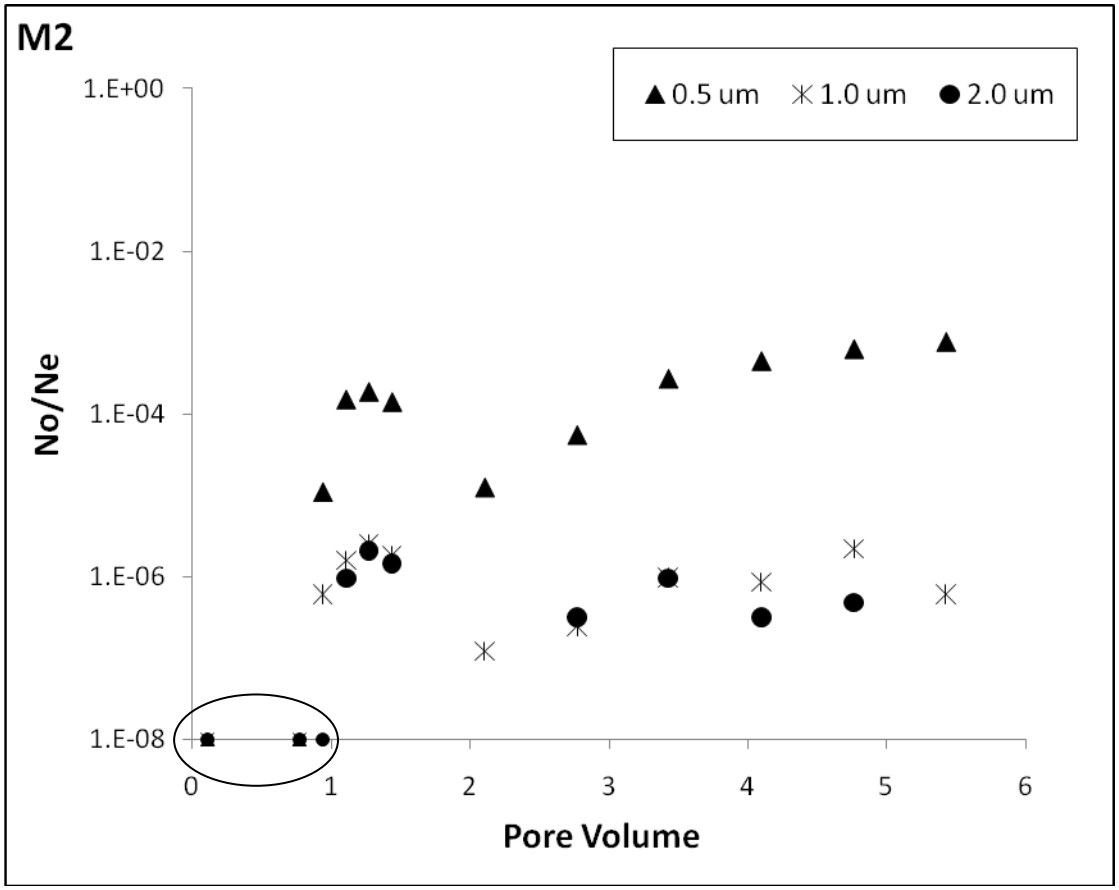


Figure A3- Results for effluent samples from surface application of microspheres experiment M2 (fine sand).
Presented as the concentration of given size microsphere normalized to the total number of that size microsphere applied to (Ne/No). Analytical results were non-detect for circled data points.

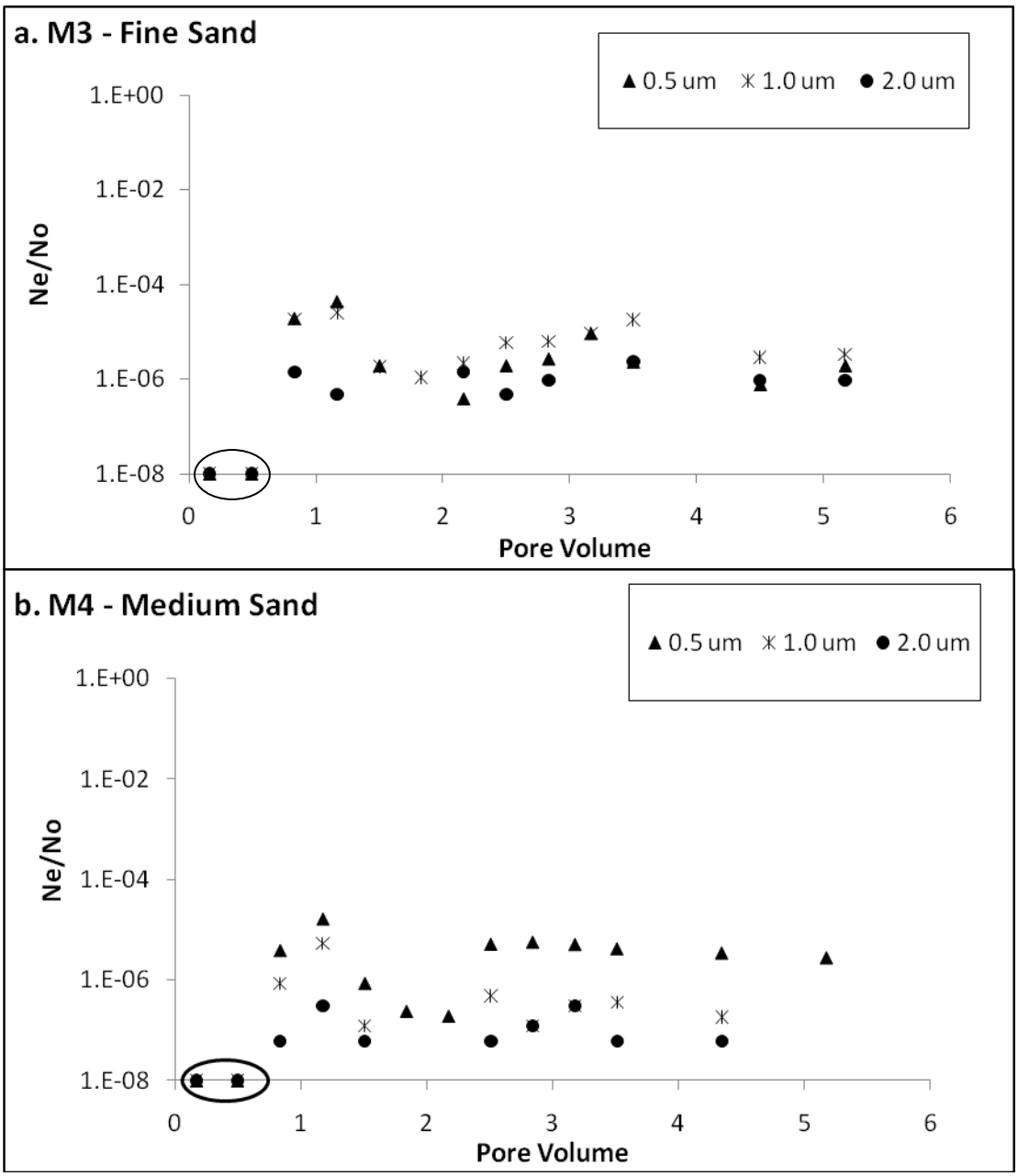


Figure A4 - Results for effluent samples from surface application of microspheres experiments M3 (fine sand) (a) and M4 (medium sand) (b).
Presented as the concentration of given size microsphere normalized to the total number of that size microsphere applied to (Ne/No). Analytical results were non-detect for circled data points.

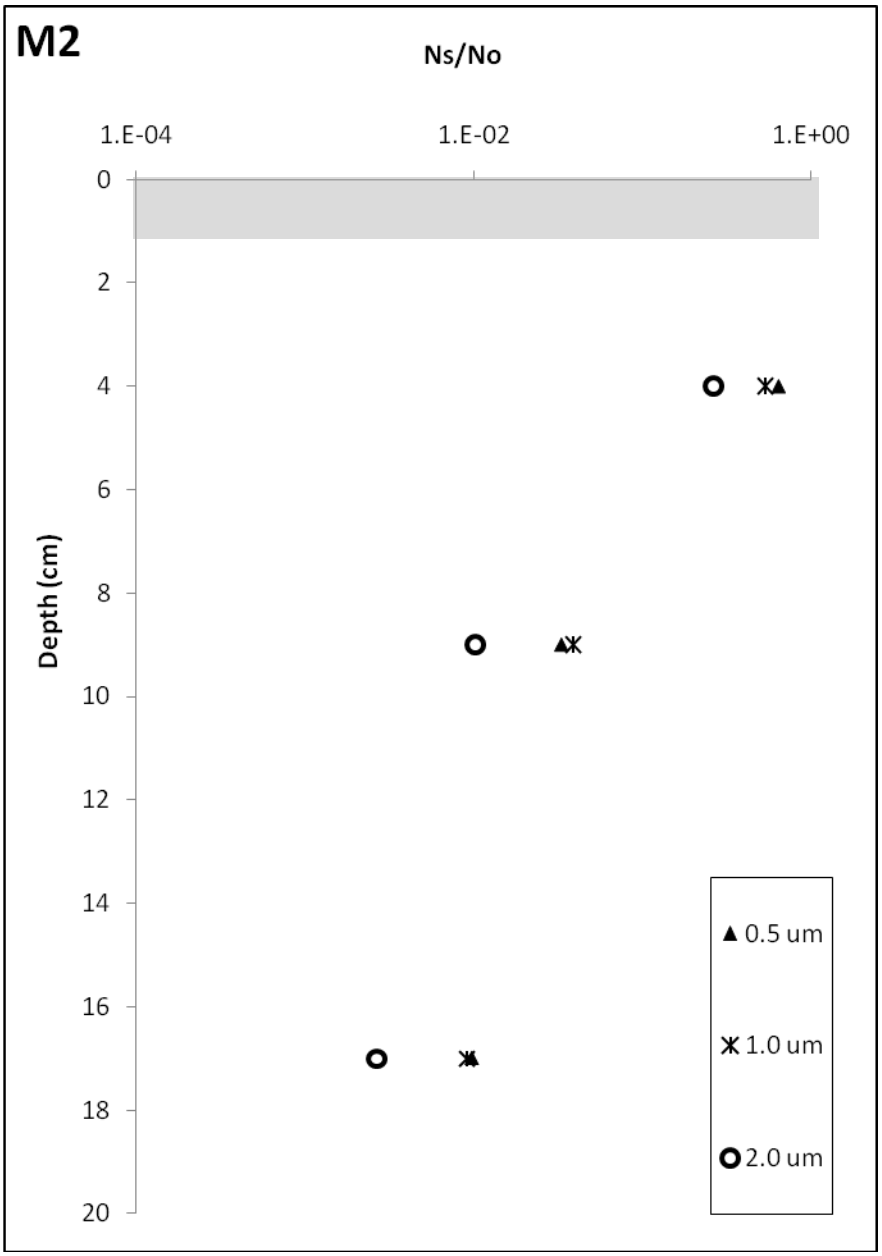


Figure A5 - Distribution of microspheres in sand samples from surface application experiment M2 (fine sand)

Presented as the concentration of a given size microspheres (Ns # of spheres/g of sand) normalized to the initial concentration of microspheres in applied to the top of the column (No # of spheres/gram of sand). Shaded area indicates depth of microsphere surface application.

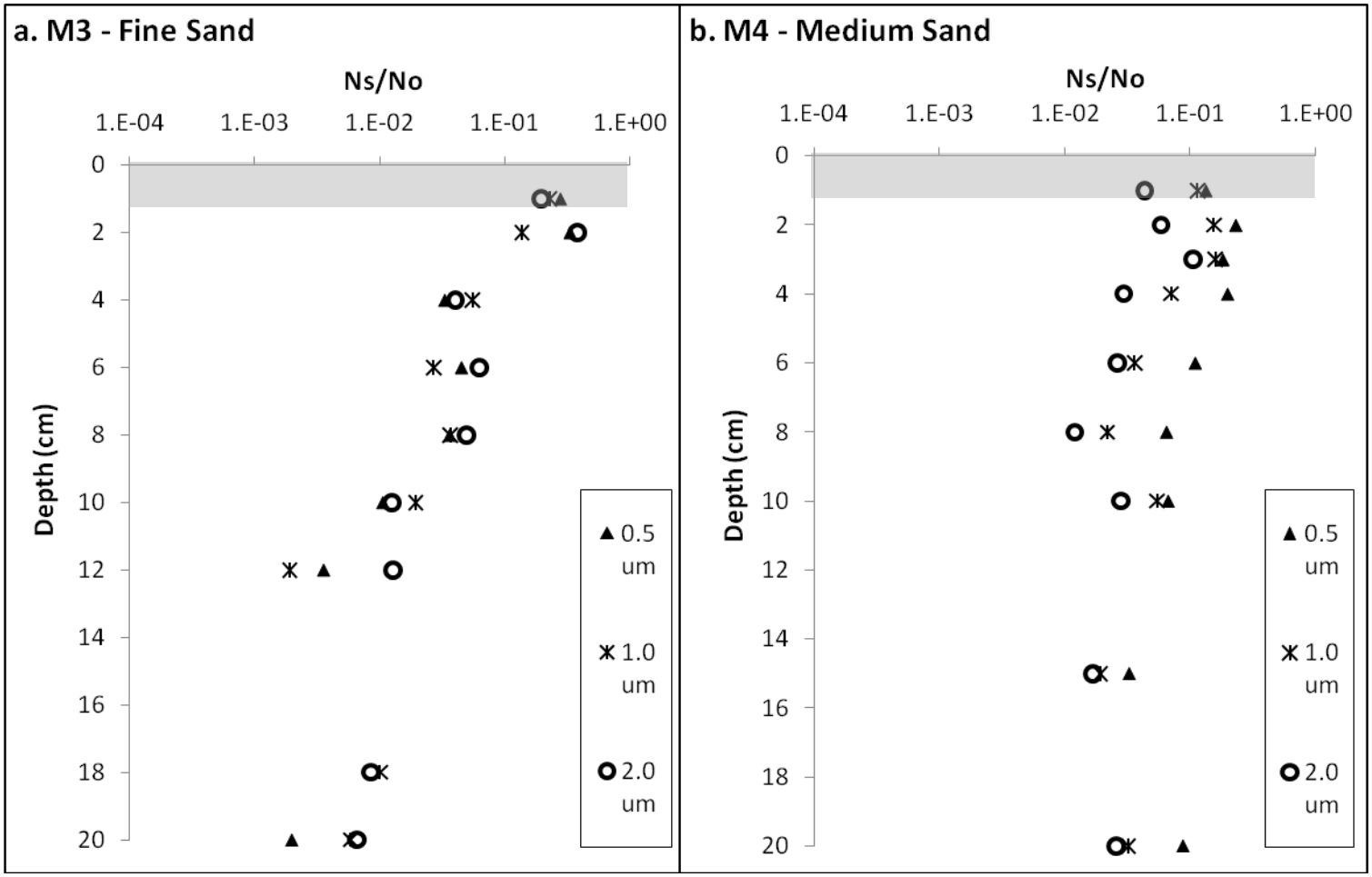


Figure A6- Distribution of microspheres in sand samples from surface application experiments M3 (fine sand) (a) and M4 (medium sand) (b).

Presented as the concentration of a given size microspheres (Ns # of spheres/g of sand) normalized to the initial concentration of microspheres in applied to the top of the column (No # of spheres/gram of sand). Shaded area indicates depth of microsphere surface application.

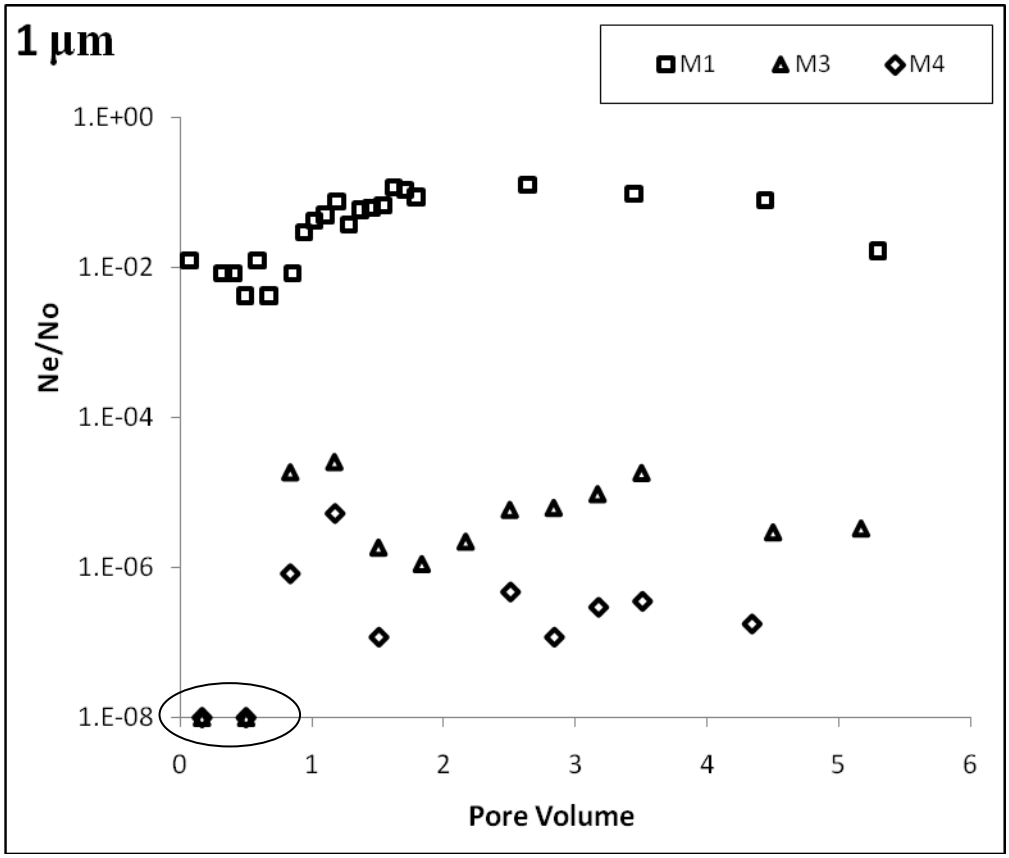


Figure A7 – A comparison of normalized 1.0 um microsphere breakthrough data for suspended microsphere experiment M1 and microsphere particulate tracer experiments M3 and M4. Analytical results were non-detect for circled data points.

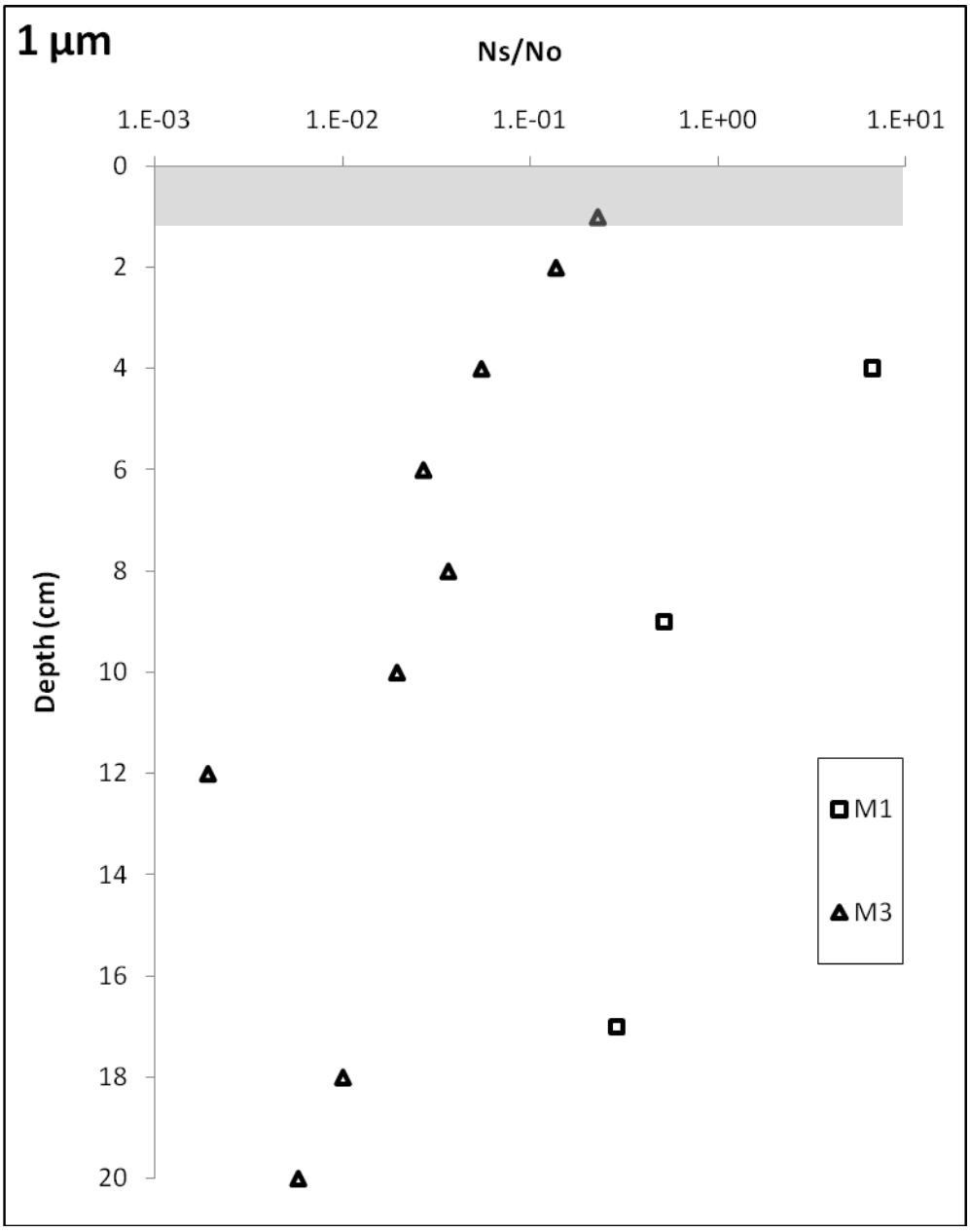


Figure A8 – Normalized distribution of 1 µm microsphere in sand samples from surface application experiment M3 and suspended experiment M1.
Shaded area indicates depth of DNT microsphere application.

Appendix B Tables

Table A1: Microsphere Log Reduction

Exp. ID	Log Removal of Microspheres		
	0.5 µm	**1.0 µm**	**2.0 µm**
M1[1]	5.E-02	2.E-01	4.E-02
M2	5.E-04	8.E-07	4.E-07
M3	2.E-06	5.E-06	6.E-07
M4	3.E-06	2.E-07	9.E-08

Removal values for each size microsphere were calculated using average plateau breakthrough concentrations normalized to influent concentrations in the reservoir.

1- 0.5 µm microspheres calculations also included 0.2 um microspheres.

Table A3 - Mass balance results for microsphere experiments

Exp.	Total Number of Spheres[1]	Percent Recovered in Effluent				Percent Recovered in Sand				Total Percent Recovered
		0.5 µm	1.0 µm	2.0 µm	Total	0.5 µm	1.0 µm	2.0 µm	Total	
M1	7.04E+06	3.6%[2]	13.5%	4.6%	21.8%	8099%[1]	200%	6.7E+05%	6.7E+05%	6.7E+05%
M2	7.6E+08	8.5%	0.02%	0.01%	8.5%	445%	379%	180%	1004%	1013%
M3	7.4E+08	0.07%	0.09%	0.01%	0.06%	116%	84%	123%	106%	106.1%
M4	5.3E+09	0.07%	0.01%	0.002%	0.009%	188%	108%	60%	78.7%	78.8%

1- For experiment M1, total number of spheres refers to estimated total number of microspheres applied to the column based on microsphere concentration detected in samples from the influent reservoir. For experiments M2, M3 and M4, it refers to the estimated total number of microspheres mixed into the top centimeter of sand in the column.

2- For M1, the 0.5 um microspheres calculations also included 0.2 um microspheres.

Appendix C

Bromide Tracer and Modeling Results

Bromide tracers were used in all transport experiments with the exception of 3F-P, 4F, 5M, and 6F. Bromide breakthrough data were modeled with CXTFIT to estimate the hydrodynamic dispersion coefficient (D). Modeling results are presented in **Table C1**. Modeled bromide breakthrough curves from transport experiments M3 and M4 are presented in **Figures C1a** and **C1b**, respectively. **Figures C2a** through **C2d**, compare bromide breakthrough curve arrival times relative to the arrival of 1 μm microspheres (for microsphere suspension experiment M1 and microsphere surface application experiments M2, M3, and M4). Bromide data are presented as concentration (ppm) normalized to the influent concentration per pore volume of effluent. Microsphere data are plotted as 1 μm sphere concentrations (# /ml) versus pore volume of effluent. In general, arrival of the 1 μm microspheres is slightly delayed relative to the bromide. Results for microsphere suspension experiment M1 suggest that the arrival of microspheres precedes the bromide by 1 pore volume. However, as previously mentioned, the microsphere data points of < 100/ml in experiment M1 are most likely background interference and not indicative of early microsphere arrival

Appendix C Figures

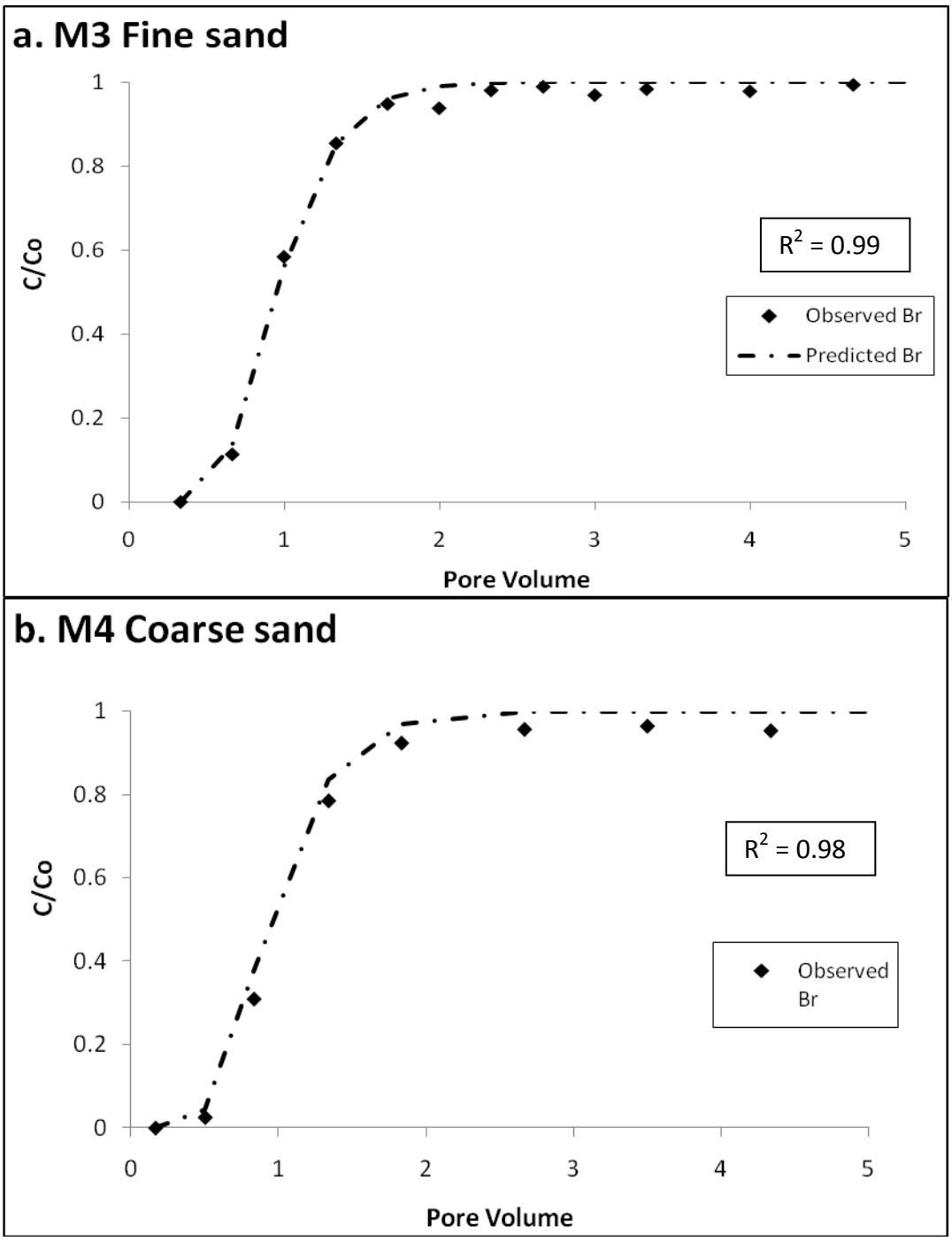


Figure C1 - Bromide data and modeling results for microsphere surface application experiments M3 (a) and M4 (b).
Presented as concentration normalized to the influent concentration (C/C_o) versus pore volume of effluent.

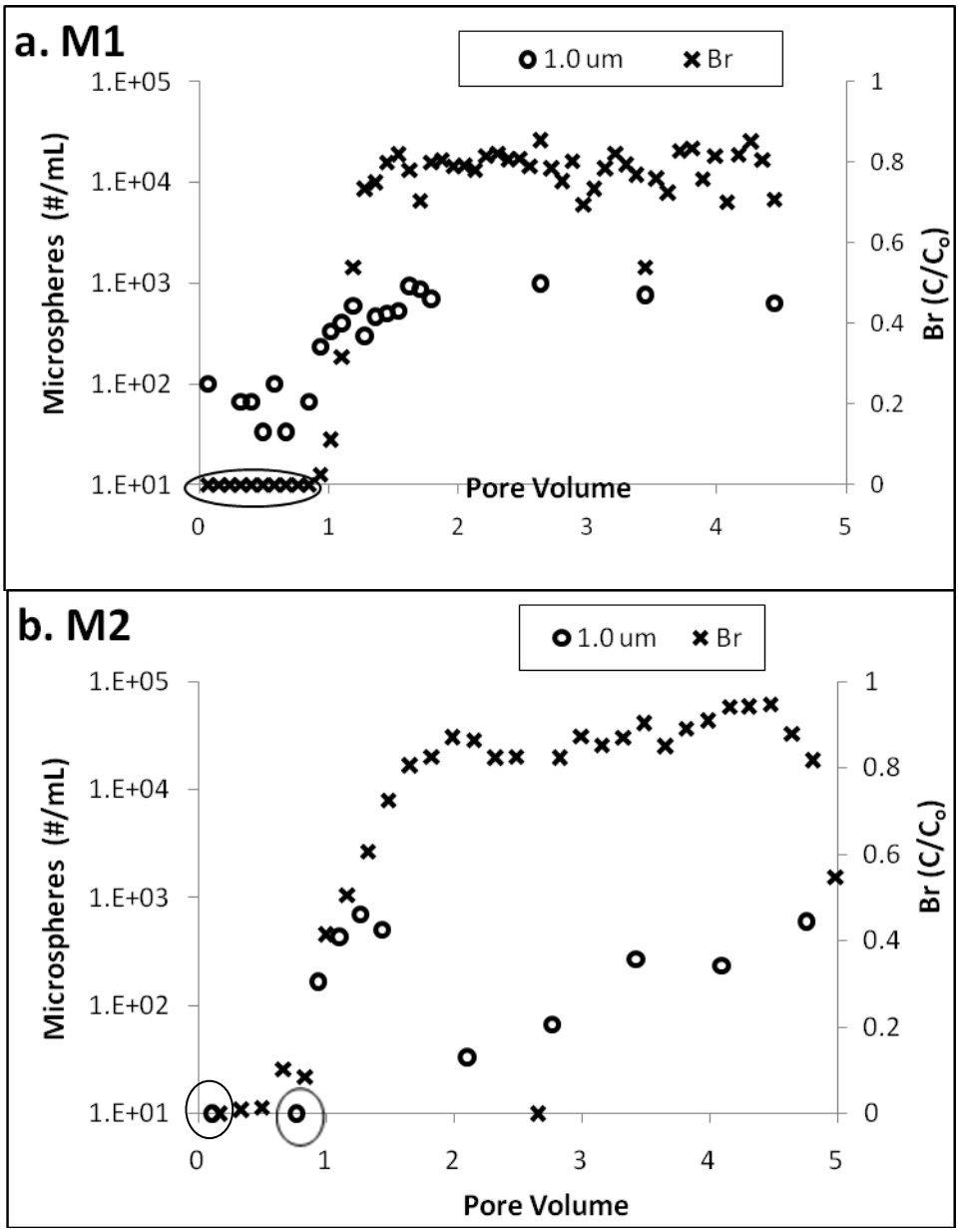


Figure C2a-b: Comparison of Br (C/Co) arrival to 1 um microsphere (#/mL) arrival.
Data from suspension experiment M1 and surface application experiment M2. Presented as Br concentration (ppm), normalized to the influent concentration (C/C_o), and 1 μm microsphere concentrations (# /ml) per pore volume of effluent. Analytical results were non-detect for circled data points.

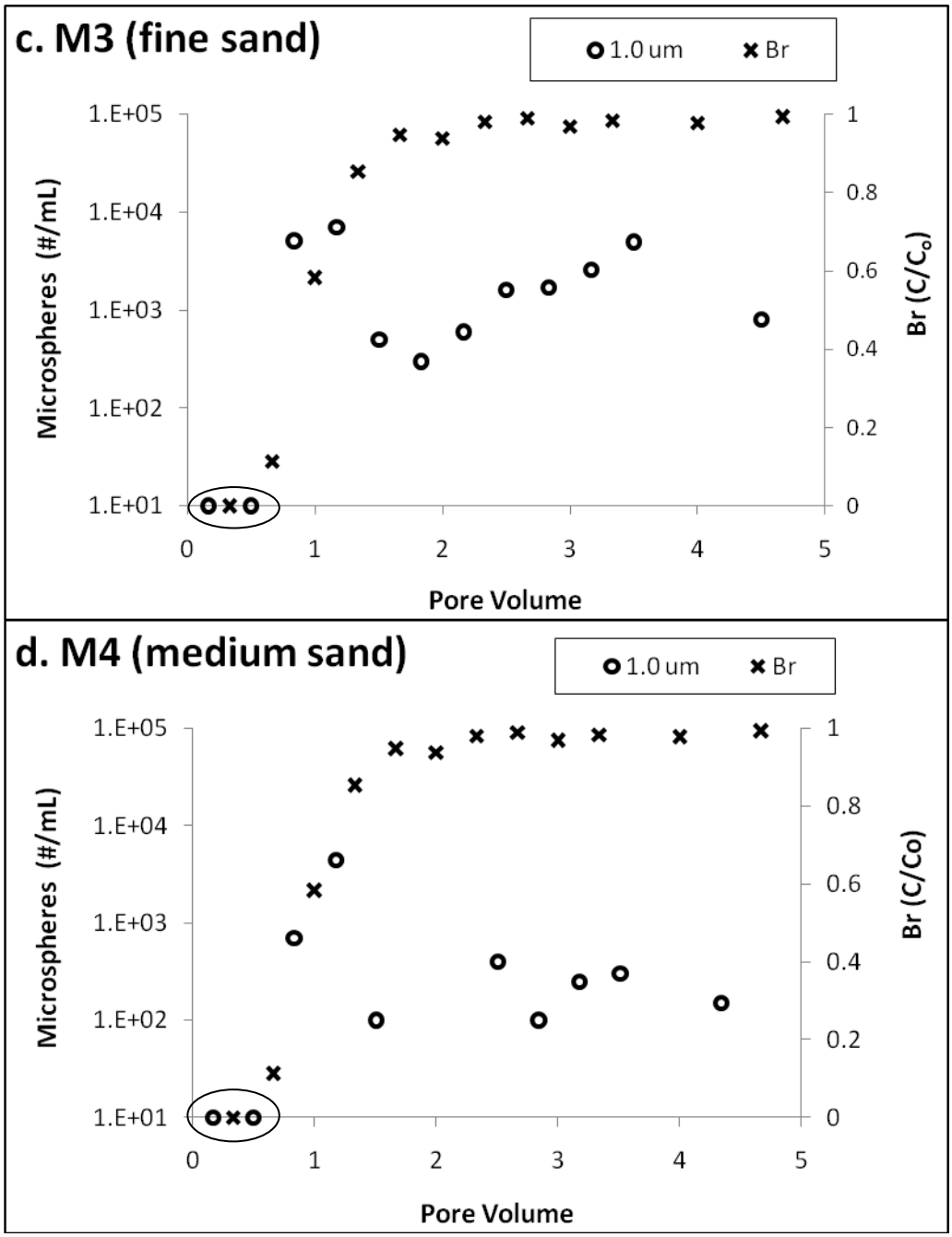


Figure C2c-d: Comparison of Br (C/Co) arrival to 1 um microsphere (#/mL) arrival.
Data from surface application experiments M3 (fine sand) and M4 (medium sand). Presented as Br concentration (ppm), normalized to the influent concentration (C/C_o), and 1 μm microsphere concentrations (# /ml) per pore volume of effluent. Analytical results were non-detect for circled data points.

Appendix C Tables

Table C1 - Modeling Results

Hydrodynamic dispersion coefficient values determined using bromide breakthrough data modeled with CXTFIT.

Modeling Results	**Transport Experiment**					
	M1	**M2**	**M3**	**1F-P**	**2F-P**	**M4**
Dispersion Coefficient (cm^2/s)	0.49	2.11	1.08	1.77	1.56	1.39
R^2	0.57	0.39	0.99	0.44	0.75	0.98

Vita

Bethsheba Lavoie was born in Madison, Wisconsin in 1975. She grew up in central New York where she attended Liverpool High School. She earned her Bachelor's in Science in Geology at Georgia State University (2007). Prior to pursuing graduate studies, she worked for an environmental consulting firm in Kennesaw, Georgia. In January of 2010, Ms. Lavoie will begin her doctorate program at the University of Tennessee, Knoxville.